MOBILITY LOAD BALANCING IN SELF-ORGANIZING OFDMA NETWORKS

by

Nur Öykü Tuncel

B.S., Electrical and Electronics Engineering, Işık University, 2012

Submitted to the Institute for Graduate Studies in
Science and Engineering in partial fulfillment of
the requirements for the degree of
Master of Science

Graduate Program in Electrical and Electronics Engineering
Boğaziçi University

2014

ACKNOWLEDGEMENTS

First, I would like to express my biggest gratitude to my advisor Assoc. Prof. Mutlu Koca for his invaluable support and guidance. I would like to thank my committee members, Prof. Cem Ersoy and Prof. Hakan Deliç for sharing their comments and profound knowledge.

I would like to thank WCL people for their help and making the time I spend in lab very enjoyable. I would also like to thank my friends who motivate and support me during the preparation of this thesis, as well as in all other aspects of my life.

Lastly, I would like to express my gratitude to my parents who have always been my truest supporters and thank them for all their love, understanding and encouragement.

This thesis is supported in part by Argela and the Turkish Undersecretariat for Defence Industries within the ULAK project framework.

ABSTRACT

MOBILITY LOAD BALANCING IN SELF-ORGANIZING OFDMA NETWORKS

In any cellular network, load imbalance results in inefficient resource utilization and low throughput for cell-edge users. Mobility Load Balancing (MLB) is an essential feature of self-organizing networks (SON) concept in long term-evolution (LTE) and introduced as a tool to balance the uneven cell load among the cells. MLB functionality changes the virtual cell borders with automatic handover parameter adjustment so that some of the load of the overloaded cells can be shifted to the less loaded neighbors. One other major problem for cell-edge users is inter-cell interference (ICI). To mitigate the ICI problem various frequency planning schemes are proposed in the scope of inter-cell interference coordination (ICIC). A significant number of studies have investigated MLB however previous solutions are isolated from ICI mitigation techniques and executed for a specific scheduling strategy. In this thesis, the performance of MLB is considered jointly with static ICIC approaches for different scheduling strategies. We evaluate the performance of MLB for different frequency planning schemes, i.e. strict fractional frequency reuse (FFR) and soft frequency reuse (SFR) using different resource scheduling strategies, i.e. round-robin, proportional fair and best-CQI. We also apply reuse-1 and reuse-3 methods to provide benchmarks while showing the gain of ICI mitigation. In the cases of FFR and SFR, the intra-cell LB mechanism is included in MLB functionality together with inter-cell MLB. Results show that static ICIC enhances MLB performance in terms of cell-edge spectral efficiency and reduces the number of unsatisfied users. Additionally, we observe the performance improvement when the non-adjacent neighbors of the overloaded cell are included in the optimization area.

ÖZET

KENDİ KENDİNE DÜZENLENEN DFBÇE AĞLARDA HAREKETLİ YÜK DENGELEME

Yük dengesizliği, tüm hücresel ağlarda hücre-kenarı kullanıcıları için verimsiz özkaynak kullanımı ve düşük veri hacmi ile sonuçlanmaktadır. Hareketli yük dengeleme (HYD), uzun dönem evrimi (UDE) içinde kendi kendine düzenlenen ağlar (KKDA) kavramının esas özniteliklerinden biridir ve hücreler arası düzensiz yük dağılımını dengelemeyi amaçlayan bir araç olarak ortaya konmuştur. HYD işlevi sanal hücre sınırlarını otomatik aktarma parametlerini ayarlayarak değiştirir, böylelikle aşırı yüklü hücrelerin yükünün bir kısmı az yüklü bitişik komşulara kaydırılabilir. Hücre-kenarı kullanıcıları için bir diğer temel problem hücreler-arası girişimdir (HAG). HAG problemini azaltmak için hücreler-arası girişim eşgüdümü (HAGE) kapsamında çeşitli frekans planlama yöntemleri önerilmiştir. Önemli sayıda çalışma HYD'yi incelemiştir buna rağmen önceki çözümler HAG azaltma tekniklerinden yalıtılmıştır ve belli bir dağıtım stratejisi için yürütülmüştür. Bu tezde, HYD başarım gelişimi sabit HAGE yaklaşımlarıyla beraber farklı dağıtım stratejileri için dikkate alınmıştır. HYD başarımını farklı frekans planlama yöntem leri için, kesirli frekans yeniden kullanımı (KFYK) ve yumuşak frekans yeniden kullanımı (YFYK) olmak üzere, farklı dağıtıcılar, round-robin, orantılı adil ve en iyi-KKG olmak üzere, kullanarak değerlendirdik. HAG azaltma kazancını gösterirken kıstas sağlayabilmek için yeniden kullanım-1 ve yeniden kullanım-3 yöntemlerine de başvurduk. KFYK ve YFYK olaylarında hücre-içi YD mekanizması HYD işlevine hücreler-arası HYD ile birlikte dahil edilmiştir. Sonuçlar gösteriyor ki sabit HAGE kullanımı HYD başarımını hücre-kenarı spektrum verimliliği açısından yükseltirken, memnun olmayan kullanıcı sayısı azaltmıştır. Ek olarak, bitişik olmayan komşular en iyileme alanına eklendiğinde başarımın arttığını gözlemledik.

TABLE OF CONTENTS

LIST OF FIGURES

LIST OF TABLES

LIST OF SYMBOLS

BW_{PRB}	Transmission bandwidth of a physical resource block
$\mathbf{c}$,$\mathbf{u}$	Coordinates of cth cell and uth user
$\mathbf{C}$	Total number of cells in the network
CIO_{max}	Upper bound of cell individual offset
CIO_{min}	Lower bound of cell individual offset
D_u	CBR requirement of user u
$F_{n,s}$	Frequency specific offset of serving cell with respect to neighboring cell
G_{cu}	Pathloss between c cell and u user
H	Hysteresis parameter
h^w_{clu}	Channel fading coefficient between cell c and user u in band w on PRB l
$J(\widehat{LOAD})_{inter}$	Inter-cell load balance index
$J(\widehat{LOAD})_{intra}$	Intra-cell load balance index
$\mathbf{K}$	Number of adjacent neighbors of a cell
$L_c(\overrightarrow{q_u})$	Position dependent pathloss between cell c and user u
$LOAD_c$	Real load of cell c
$LOAD_{th}$	Overload threshold
$LOAD_{th,HO}$	Load threshold for handover operation
$\widehat{LOAD}_c$	Virtual load of cell c
$\widehat{LOAD}_{env,i}$	Environment state of cell i
$\widehat{LOAD}_{ij}$	Virtual load of jth adjacent neighbor of cell i
$\widehat{LOAD}_{over,i}$	Overall state of cell i
$\widehat{LOAD}^{est}_{u,TeNB}$	Estimation of load created in target eNB by user u
$\widehat{LOAD}^w_c$	Virtual load of band w in cell c
N_{int}	Number of PRBs allocated for inner band
N_{out}	Number of PRBs allocated for outer band
$N_{tot,c}$	The total number of PRBs reserved for cell c
$N^w_{tot,c}$	Total number of PRBs reserved for band w in cell c

N_u	Number of PRBs scheduled for user u
$\widehat{N_u}$	Number required PRBs to serve user u
$\widehat{N_{c,u}^w}$	Number required PRBs to serve user u from cell c in band w
$O_{n,s}$	CIO of serving cell with respect to neighboring cell
$\overrightarrow{q_u}$	position of user u
Q_c^w	Set of cells that use band w as cell c
P_c	Downlink transmitted power of cell c
P_{cl}^w	Downlink transmitted power of cell c on PRB l in band w
R_s	RSRP measured by serving cell
R_n	RSRP measured by neighboring cell
$R\,[SINR_u]$	Bandwidth efficiency of user u per PRB
$R\,[SINR_{clu}^w]$	Bandwidth efficiency of user u from cell c in band w on PRB l
$R\,[SINR_{cu}^w]$	Average bandwidth efficiency of user u from cell c in band w
$R_{int,c}$	Radius of interior region of cell c
$R_{int,c}^{temp}$	Temporary value of radius of interior region of cell c
S_c^w	The set of PRB of cell c in band w
$SINR_{th,min}$	Minimum SINR value that is not cause radio link failure
$SINR_u$	Signal to interference plus noise ratio of user u per PRB
$SINR_{TeNB,u}^{est}$	Estimation of SINR received by user u from target eNB
$SINR_{clu}^w$	SINR of user u from cell c on PRB l in band w
$TeNB_{temp}$	Temporarily chosen target eNB
$\mathbf{U_c}$	The set of CBR users connected to in cell c
$\mathbf{U_c^w}$	The set of CBR users connected to cell c assigned to band w
$\mathbf{W}$	Set of all bands
w_T	Sub-band assigned to target eNB
Z_c	Number of unsatisfied users
Δ_{intra}	Increment steps for interior radius
α	Pathloss exponent
μ	Measure of influence of virtual load state on the overall load state

ρ_z	The fraction of used PRBs in cell z
σ^2	Noise power

LIST OF ACRONYMS/ABBREVIATIONS

1G	1st Generation
2G	2nd Generation
3G	3rd Generation
3GPP	3rd generation partnership project
AMC	Adaptive modulation and coding scheme
CAC	Composite available capacity
CAPEX	Capital expenditure
CBR	Constant bit rate
CCC	Cell coverage control
CIO	Cell individual offset
CQI	Channel quality indicator
DM	Domain manager
ECDF	Empirical cumulative distribution function
eNB or eNodeB	Evolved node B
EPC	Evolved packet core
EPS	Evolved packet system
E-UTRAN	Evolved universal terrestrial radio access network
FFR	Fractional frequency reuse
FSO	Frequency specific offset
GSM	Global system for mobile communications
HO	Handover
HPC	Handover parameter control
HSPA	High speed packet access
HSPA+	High speed packet access evolution
ICI	Inter-cell interference
IE	Information element
IP	Internet protocol
KPI	Key performance indicator
LA	Link adaptation

LB	Load balancing
LTE	Long term evolution
MCS	Modulation and coding scheme
MLB	Mobility load balancing
MME	Mobility management entity
MRO	Mobility robustness optimization
NE	Network element
NGMN	Next generation mobile networks
NMLB	Neighborhood mobility load balancing
OAM	Operation, administration and management
OFDM	Orthogonal frequency division multiplexing
OFDMA	Orthogonal frequency division multiple access
OPEX	Operation expenditure
PAPR	Peak-to-average power ratio
PDN	Packet data network
PDN-GW	Packet data network gateway
PRB	Physical resource block
RAT	Radio access technology
RRM	Radio resource management
RSRP	Reference signal received power
RSRQ	Reference signal received quality
SC-FDMA	Single carrier frequency division multiple access
SeNB	Source eNB
SFR	Soft frequency reuse
SINR	Signal to interference plus noise ratio
SON	Self-organizing networks
S-GW	Serving gateway
TeNB	Target eNB
UE	User equipment
UMTS	Universal mobile terrestrial system
TTI	Transmission time interval

TTT	Time-to-trigger
VoIP	Voice over IP
WCDMA	Wideband code division multiple access

1. INTRODUCTION

Number of mobile broadband subscribers and data traffic grows exponentially over the last few years. This growth implies increasing demand for known and new data services. To be able to satisfy customer requirements, operators need to upgrade their networks and use the resources more effectively. Long Term Evolution (LTE) is one of the latest cellular network technologies which brings improved system capacity, good coverage, higher bandwidth efficiency and reduced cost for operators as stated in [1]. LTE has a flat and internet protocol (IP) packet based architecture that minimizes the number of network elements and latency. LTE requirements have developed and standardized by the international standardization body the Third Mobile Generation Partnership Project (3GPP) and operators lobby Next Generation Mobile Networks (NGMN).

Operators face significant operational challenges in terms of operational cost and manual work while they are trying to reach the LTE requirements and standards. The manual work and human intervention cause delay and erroneous decisions. The concept of self-organizing network (SON) has developed to minimize the delay and errors by reducing manual workload and automation of planning and configuration functionalities. Along with SON, the role of human has shifted from time consuming frequent routine tasks to pure monitoring and supervision. SON enabled networks have three major sub-functionalities: self-configuration, self-optimization and self healing. Self-configuration involves the operations applied in the automatic installation of the newly added network elements. Self-optimization is the mechanism that optimizes the parameters of the network based on the collected measurement reports. Finally, self-healing is the process of automatic detection and recovery of network failures.

In LTE networks, the volume of traffic between particular points fluctuates over time and space. Consequently, some cells becomes overloaded, whereas some others are less loaded. The term load balancing (LB) is to direct the excessive load from overloaded cells to low loaded cells by reducing the coverage area of high loaded cell and

increasing the coverage area of their less loaded neighbor cells simultaneously. There are two ways of re-distribution of load between cells. One approach is changing the downlink transmit power of the cell and second approach is modification of handover (HO) regions between adjacent neighbors by changing HO parameters automatically. Second approach refers mobility load balancing (MLB) which is one of the features of self-optimization functionality. Adjustment of HO offset parameters changes virtual cell borders and triggers HO operation for users that locate on cell-edge. This operation provides more efficient radio resources usage across the whole network and as a result, the number of low throughput users is reduced.

LTE uses orthogonal frequency division multiple access (OFDMA) which is well suited to achieve high peak data rates, low latency and improved spectral efficiency for downlink transmission. In this context, appropriate resource scheduling plays an important role in order to meet the system performance targets and satisfy user requirements. The scheduling algorithm impacts the throughput of individual users as well as throughput of the cell significantly. Additionally, OFDMA networks supports intra-cell orthogonality, that is the users served by the same base station do not receive/create interference on each other [2]. However, when a multi-cellular network is considered, heavy inter-cell interference (ICI) between neighboring cell is induced and ICI is one of the major factors that degrades system performance, especially for cell-edge users. In order to mitigate ICI, various frequency planning schemes which suggests reusing and dividing the total bandwidth are proposed.

1.1. Scope of the Thesis

There have been lots of studies which investigate MLB solutions, static ICIC approaches and scheduling strategies individually. To the best of our knowledge, there is no research done which considers MLB for all static ICIC approaches and also compare the performance of MLB for different scheduling strategies. On the other hand, there are limited number of studies which consider LB in an FFR network. However these limited studies solve the LB problem in a heuristic method without taking the MLB handover parameter adjustment into account. The main contribution of this work is to

combine MLB functionality with frequency planning schemes which are in the scope of static ICIC approaches and compare MLB performance for different scheduling strategies. In this dissertation, we evaluate the MLB performance for most commonly used frequency planning schemes, i.e. FFR and SFR using different scheduling approaches presented in the literature, i.e. round-robin, proportional fair and best-CQI. We also simulate MLB for reuse-1 and reuse-3 to create benchmarks while observing the efficiency of ICI mitigation techniques. In the cases of reuse-1 and reuse-3, MLB implies inter-cell LB whereas in the cases of FFR and SFR, MLB refers coordination of inter-cell and intra-cell LB. According to the 3GPP standards, only adjacent neighbors of the overloaded cell are involved in LB operation. However, we also observe the affect of including the non-adjacent neighbors of the overloaded cell in the optimization area of LB operation and compared with the method defined in the standards. Results show that performance of MLB is improved with the help of ICI mitigation techniques in terms of reduction in the number of unsatisfied users and improvement in the cell-edge user spectral efficiency. On the other hand, in some cases where the adjacent neighbors have not enough available capacity to offload the overloaded cell adding the non-adjacent neighbors into the LB operation improves the performance gain.

1.2. Outline

The rest of the thesis is organized as follows. In Chapter 2 main system requirements, system architecture of LTE is overwieved with SON concept and also a brief introduction about MLB functionality is given. In Chapter 3 main scheduling strategies used in LTE and static ICIC approaches are detailed. In Chapter 4, we present how MLB is considered jointly with static ICIC approaches and in Chapter 5 we give the simulation results. Finally, in Chapter 6, we conclude the thesis.

2. LTE OVERVIEW

LTE is a 3GPP project and created as an extension of universal mobile telecommunications system (UMTS). LTE offers higher data rate, reduced latency and simplified network architecture compared to its predecessor technologies. LTE requirements and standards are specified in release 8 document series of 3GPP and enhanced in the further releases, release 9, 10 and 11 with some additive features. Before giving the technical and functional details of LTE, we present a brief historical background and basic requirements.

The first cellular network is introduced in early 1980s and the development of mobile communications has divided into phases and generations with the aim of better performance, capacity, higher data rate, wider coverage and lower cost as in [3]. First generation (1G) refers to analog cellular technologies and used for only voice calls. In 1992, a new generation called 2G which provides purely digital technology was developed. 2G provides higher data throughput up to 14.4 kpbs for voice communication and messaging. Global system for mobile communications (GSM) is the standard which describes the protocols used in 2G. GSM was developed by 3GPP which was formed by the European telecommunications standards institute. In late 90's, the demand for packed data dominated mobile networks has increased. However, GSM mainly supports voice traffic and some other data capability is added subsequently. The third generation (3G) mobile system was developed by 3GPP in 1998 in order to satisfy the increasing demand for packet data traffic. In 3G, high speed packet switching capability is provided besides circuit switched voice transmission. It is based on wideband code division multiple access (WCDMA) with 2 Mbps peak data rate in downlink and 1 Mbps at the uplink, high speed packet access (HSPA) and its enhancements HSPA Plus (HSPA+). Web browsing, email, video downloading, picture sharing and other smart phone technology were introduced in 3G.

The need for even higher data rate and the usage of 'always on' and 'everywhere' devices such as smart phones, tablets, location-based/personal navigators make it cru-

cial to find a new radio access technology (RAT) with a new network architecture in the longer term. LTE is the evolutionary technology which provides even higher data rate and lower latency, standardized by 3GPP. Unlikely to its predecessors, LTE has a completely packet switched core network architecture and both IP data traffic and voice services are supported over the same packet switched network, i.e. voice over IP (VoIP) as in [4].

LTE requirements were defined in the first half of 2005. LTE allows flexible bandwidth ranging from 1.4 MHz to 20 MHz. LTE supports a new air interface OFDMA to reach peak transmission rate of 100 Mbps in the downlink and supports single carrier FDMA (SC-FDMA) to reach 50 Mbps in the uplink [5]. Spectral efficiency values of 5 bits/s/Hz and 2.5 bits/s/Hz for UL and DL respectively within a 20 MHz bandwidth. The cell coverage is 5 to 100 km with slight deterioration after 30 km.

2.1. LTE System Architecture

The requirements of LTE lead the definition of a new network architecture namely evolved packet system (EPS) according to the [9]. EPS aims to provide IP connectivity between user equipment (UE) and the packet data network (PDN). EPS uses the concept of EPS bearers which is associated with quality of service (QoS). Multiple bearers can be established for users with multiple services where each service is mapped to a different bearer. For instance, one user can be engaged with a voice call through VoIP and can browse a web page using hypertext transfer protocol or download a file using file transfer protocol at the same time. The previous systems, i.e. UMTS and GSM, have one centralized controller node responsible for controlling the base stations which is called as the radio network controller in UMTS and the base station controller in GSM. Unlike to the previous systems, LTE has a flat network architecture and all radio functionalities are integrated into one network element called as evolved Node B (eNodeB or eNB), the controllers are not needed.

EPS can be divided into two main high level domains, these are evolved universal terrestrial radio access network (E-UTRAN) and evolved packet core (EPC). The func-

tional split of the EPC and E-UTRAN structure is illustrated in Figure 2.1. E-UTRAN consists of interconnected eNodeBs. eNodeBs communicate with each other through X2 interface and with core network through S1 interface. The E-UTRAN protocols have user plane and control plane. The actual user data is transferred through the LTE network by user plane protocols. User plane protocols related with the physical layer, the medium access control layer and the packet data control protocol layer. On the other hand, the control plane protocols control and establish connections between UEs and E-UTRAN providing radio resource management, call admission control and scheduling functionalities. The core network, EPC, aims to support the users and es-

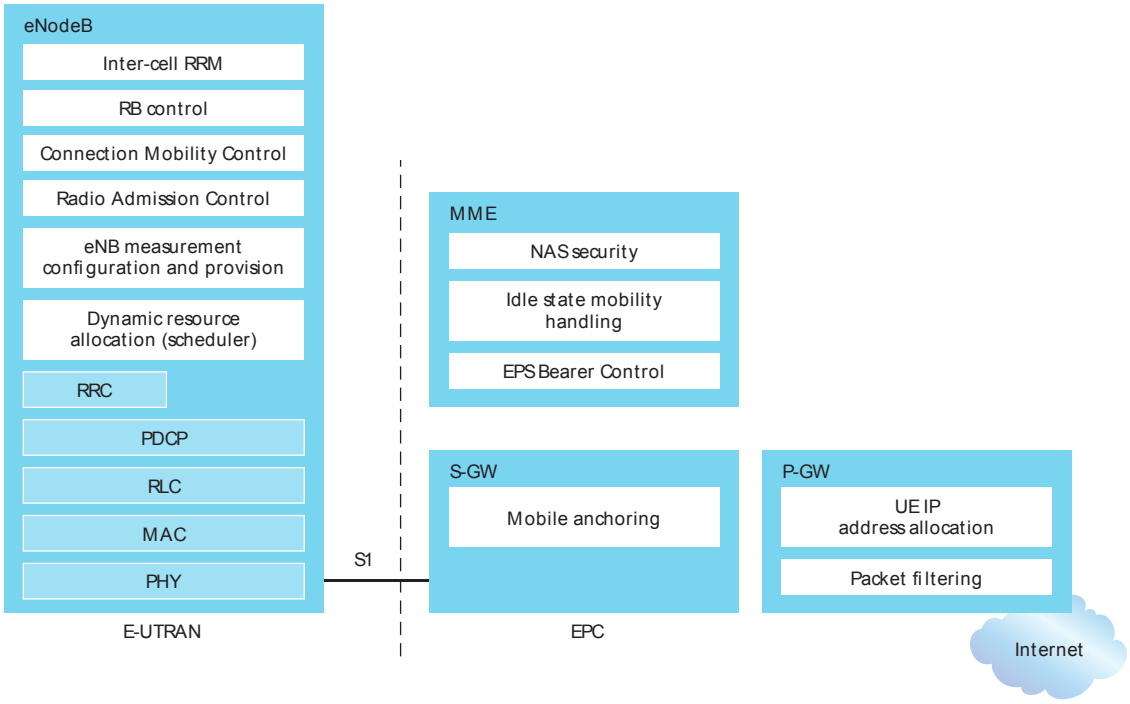

Figure 2.1. Functional split of E-UTRAN and EPC [6].

tablish their QoS associated bearers [10]. It consists of three main elements: mobility management entity (MME), serving gateway (S-GW) and the packet data network gateway (PDN-GW). MME is the central and main signalling element of EPC and optimized for control plane. MME connects to the eNBs in its serving area and paging messages through S1-MME interface. MME takes role in authentication, security, roaming, bearer establishment, idle mobility and handover functionalities. MME is responsible for ciphering and integrity protection of non-access-stratum signalling. NAS

protocols are used session management procedures and IP connectivity between UEs and packet data network gateway (PDN-GW) through MME. The other important feature of MME is the idle mode mobility. MME stores the location of the UEs in terms of UE tracking area or connected cells. When handover procedure is requested, MME directs the user-plane path from old the eNB to new the eNB. Mobility can be achieved between nodes of different 3GPP core networks. Bearer management and bearer establishment are also done by MME.

S-GW is the user plane gateway to the E-UTRAN. All user IP packets are transferred through S-GW and directed to the correct elements in the network. S-GW is an anchor point for mobility between LTE network and the other 3GPP technologies such as 2G, 3G systems. When a UE handover form one eNB to another, MME instructs S-GW to switch the user plane through new eNB. If the new eNB is not in the service area of serving S-GW, MME selects a new S-GW. When UE is in idle mode, S-GW buffers the incoming downlink data until MME starts paging. S-GW is also responsible for forwarding and routing data packets.

P-GW is the user plane gateway to the PDN. IP address allocation to the UE is done by P-GW. The incoming IP packets are mapped to the correct bearers in EPC and the services requiring different QoS are identified by packet filtering functionality of P-GW.

2.2. Multiple Access Techniques

In LTE, transmission is based on multiple access technologies. OFDMA which is the extension of OFDM has been selected for uplink transmission and SC-FDMA has been selected for downlink transmission. In this section, the certain characteristics and main advantages of OFDM, OFDMA and SC-FDMA schemes are presented.

2.2.1. OFDM

OFDM is a frequency division multiplexing scheme that transmits signals through multiple carriers. The benefits of OFDM are its robustness over frequency selective channels and higher spectral efficiency.

In order to transmit data at high rates, a wider transmission bandwidth is required as stated in [6]. When the transmission bandwidth is larger than the coherence bandwidth of the channel, the channel is no longer flat across the frequency band and faces with frequency selective fading where the different frequency components of the signal experience different uncorrelated fading. In UMTS, this problem is avoided by equalization but equalization is a complex method. Alternatively in OFDM, total transmission bandwidth is divided into large number of narrower and closely spaced sub-channels (sub-carriers). The data is carried on these sub-channels in parallel and modulated according to the selected modulation scheme e.g. QPSK, 16-QAM or 64 QAM. Since the bandwidth of a subcarrier is narrower than the coherence bandwidth of the channel, the fading becomes flat across each subcarrier [8]. The other benefit of using OFDM is channel utilization. In OFDM, the sub-carriers are orthogonal to each other therefore additional guard band intervals between sub-channels are not needed. In this way, channel is utilized more effectively without interference. Figure 2.2 is the representation of key features of OFDM signal in the joint time-frequency domain.

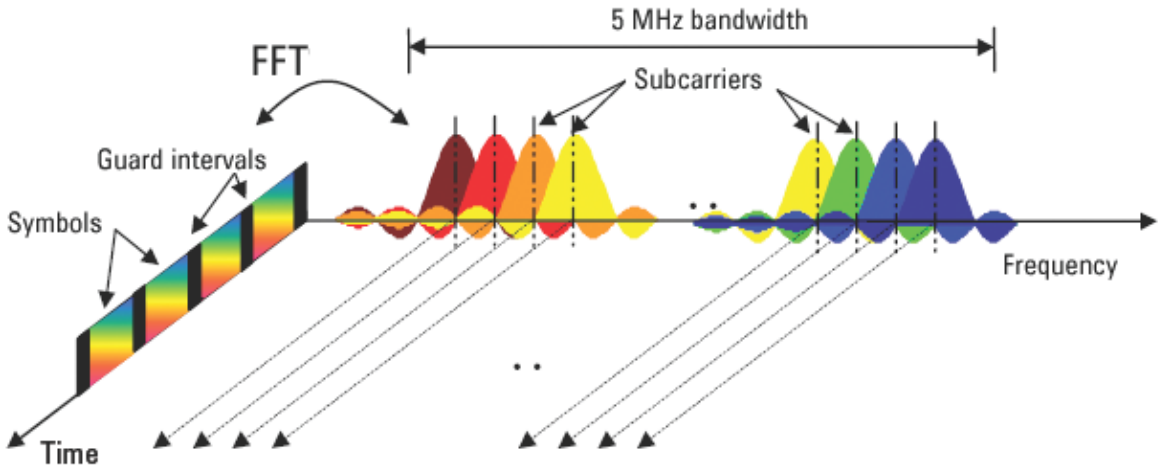

Figure 2.2. OFDM signal represented in frequency and time [11].

2.2.2. OFDMA

OFDMA is the multi user version of OFDM where the subcarriers are distributed to different users in order to support multiple users simultaneously. The subcarriers are grouped and dynamically allocated to the users so that a specific subcarrier can be allocated to a specific user for a specific time interval as shown in Figure 2.3. The smallest resource unit that can be assigned by a scheduler is called as a physical resource block (PRB). A PRB consists of 12 adjacent subcarriers where subcarrier spacing is standardized as 15 KHz. Assuming normal cyclic prefix length, one PRB occupies 180 KHz in frequency domain and consists of 7 OFDM symbols in a time slot (0.5 ms). Total number of PRBs depends on total bandwidth of the system. For example, for a 10 MHz transmission bandwidth, there are approximately 50 PRBs with 10% of the bandwidth is reserved for the guard interval.

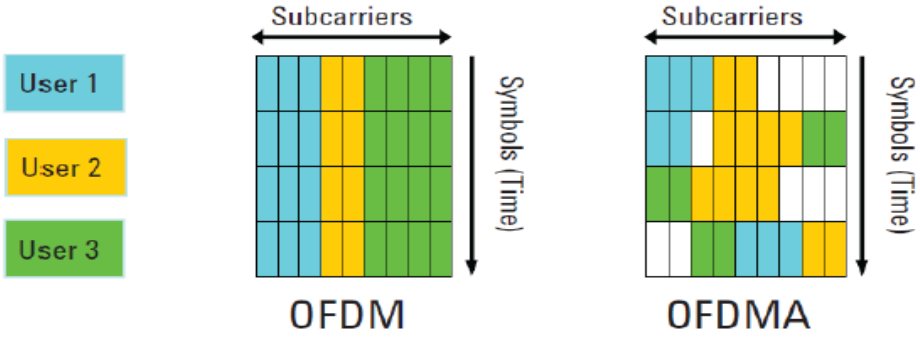

Figure 2.3. OFDM and OFDMA subcarrier allocation [11].

2.2.3. SC-FDMA

OFDMA have large variations in the instantaneous power of transmitted signal due to multi carrier transmission and it results with high peak to average power ratio (PAPR). High PAPR reduces the power amplifier efficiency and increase the mobile terminal power consumption. Therefore, OFDMA is not an ideal solution for uplink transmission as stated in [7]. SC-FDMA is the modified version of OFDMA and offers low PAPR and reduced cost for power amplifier. In SC-FDMA, single carrier transmission is implemented. Instead of dividing the total bandwidth and assigning

the resulting sub-bands to each subcarrier, SC-FDMA distributes the information bits to the subcarriers sequentially. Thus the power difference between sub-carriers is reduced. Furthermore SC-FDMA also offers the same degree of multipath protection as OFDMA.

2.3. LTE and SON

In existing communication technologies UMTS and GSM, the network parameters are configured manually. Manual intervention is inefficient, results in long delays, human errors and also creates operational (OPEX) and capital expenditures (CAPEX). LTE suggests higher capacity and QoS, in addition, it operates different 3GPP technologies (2G, 3G, LTE) in parallel. These additional requirements aggravate the complexity of network and quantity of the parameters to be optimized. In order not to face with increasing OPEX and CAPEX, the operation, administration and management (OAM) should be done very carefully. The problem is solved with the SON concept which improves the performance of the network in a cost effective manner. SON functionality reduces the manual workload in both planning and the operation phase of network management by increasing automation in the network elements (NE), domain manager (DM) and/or management system.

LTE SON requirements were initially developed according to the NGMN alliance which is created by a group of operators in 2006 given in [14]. The objective of NGMN is to provide business requirements and use cases to the new technologies being developed. NGMN use cases have been adopted to the LTE SON standardization by 3GPP from the first release of LTE, release 8, and expended in the scope of subsequent releases. In release 8, the commercial deployment of first LTE networks is considered and the focus is on installation of equipments. Release 9 is related with optimization procedures of already commercialized networks and in release 10 the existing use cases are enhanced. Release 11 and other subsequent releases cover the aspects of multi-layer and multi-RAT heterogeneous networks, network management and troubleshooting.

2.3.1. SON Functionalities

SON use cases determine the functionalities which are achieved after self organization. According to use cases, main SON functionalities can be categorized as self-configuration, self-optimization and self-healing [15].

(i) *Self Configuration:* Self configuration is a process that minimizes the human intervention in the planning and deployment phases of a new NE. Self configuration steps are: auto connectivity setup, auto commissioning and dynamic radio configuration. Once an eNB is installed and switched on, auto connectivity setup provides secure connection between eNB and the OAM system of the network. In the auto commissioning step, the required software is downloaded. Based on the downloaded data in commissioning step, NE adapts itself to the current state of the network deployment dynamically in dynamic radio configuration step. According to the [16] main self configuration use cases are; automatic neighbor relation function, automated configuration of physical cell ID.

(ii) *Self Optimization:* Self optimization is the mechanism which optimizes the operational parameters according to changing network conditions. During the operation, every eNodeB collects the measurements about the network conditions and an external tool adjusts the parameters based on measurement reports in order to achieve optimum system performance. Self optimization functions are included in release 9 and the main use cases are coverage and capacity optimization, energy saving, mobility robustness optimization (MRO), MLB and ICIC.

(iii) *Self Healing:* Self healing mechanism automatically detects and localizes the failures in the network. If any NE does not execute its actual functionality because of a fault, the NE cannot offer service and the network performance is degraded until the fault is detected and solved. Self healing function continuously monitors the network. Alarms and key performance indicators (KPIs) are used to trigger the healing process. If an alarm or an inappropriate KPI is detected, root cause of the fault is analyzed and an appropriate recovery action is selected to solve the fault automatically. Steps involved in the self healing procedure has been suggested in [17] for 3GPP.

2.3.2. SON Architecture

SON functions can reside at NM, DM or NE levels. According to the location that the optimization algorithms reside, SON architectures can be divided into four classes: centralized SON, distributed SON, localized SON and hybrid SON as detailed in [1]. In Figure 2.4 centralized and distributed SON architectures and in Figure 2.5 localized and hybrid SON architectures are depicted.

(i) *Centralized SON:* In centralized SON architecture, all optimization algorithms are stored and executed at the NM level or in the OAM system. Centralized approach is easy to deploy and has less complexity in management tasks. On the other hand, there are some drawbacks of centralized SON. In centralized approach, SON functions reside in small number of locations and decisions are made in central NEs. If there is a failure in any central NE, overall network has a risk of being affected. In addition, different vendors have different OAM systems and optimization among different vendors is not supported. The Itf-N interface which facilitates multi-vendor management should be extended and standardized in order to coordinate different vendors. Lastly, centralized SON elements collect and analyze enormous amount of data, therefore the optimization response is slow.

(ii) *Distributed SON:* In distributed SON, algorithms are executed in low level NEs, i.e. access network elements or eNBs. Different eNBs exchange information via X2 interface. Information exchange and coordination of the nodes are difficult tasks when a large number of eNBs are involved in a complex optimization problem. On the other hand, for small number of eNBs, it is easy to achieve convergence quickly and the response time is smaller comparing to centralized solution. In distributed architecture, SON functionalities reside in many locations and it causes higher deployment cost and work.

(iii) *Localized SON:* In localized architecture, the process is executed in a single cell independently from neighboring eNBs. The cooperation between eNBs is not needed therefore signaling overhead is not observed and the delay is very low. Localized architecture works multi-vendor specific and does not require any stan-

dardization.

(iv) *Hybrid SON:* The mentioned architectures types have their benefits and drawbacks. The hybrid architecture proposes a new approach which utilizes all three approaches simultaneously. In hybrid SON, some functionalities are executed in the OAM system and other functionalities are executed in low management level, eNBs. Complex optimization tasks which allow flexibility and delay are implemented in OAM whereas the tasks that need faster response implemented in the eNBs. Both X2 and Itf-N interfaces are used for multi-vendor communication and information exchange.

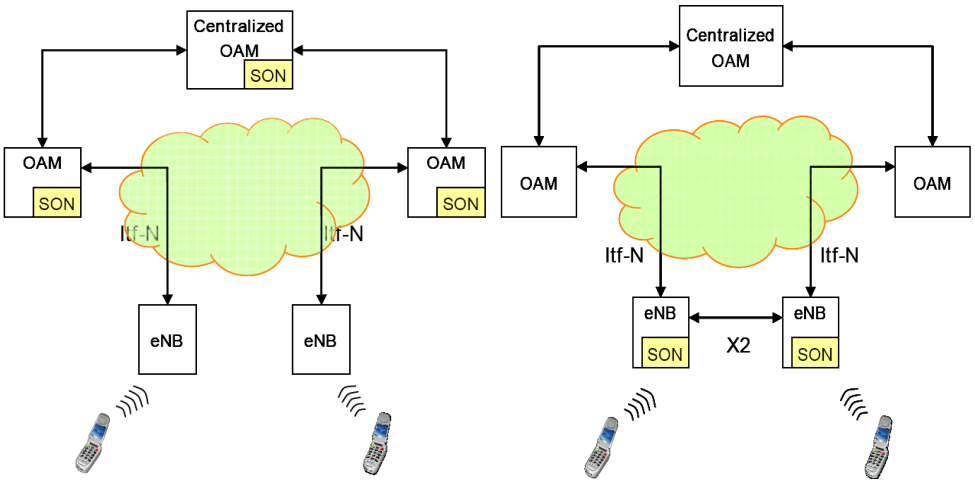

(a) Centralized (b) Distributed

Figure 2.4. Centralized and distributed SON architectures [18].

2.4. Mobility Load Balancing

In cellular networks, the arrival of mobile users is random and time varying therefore the load created in the cells are often uneven. As described in [1], MLB is one of the self-optimization use cases which aims to balance the uneven cell load among the cells which reside in a certain geographical area. In 2G and 3G LB has been done in the network planning phase or later by manual optimization. In LTE, SON policies for LB are rather dynamic and provide automatic adjustments of the mobility configurations at certain nodes based on the knowledge of load conditions

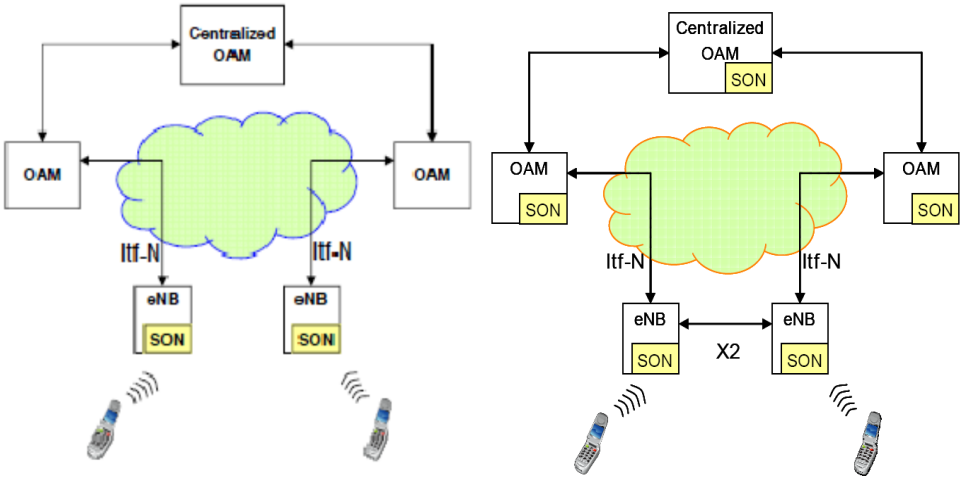

(a) Localized (b) Hybrid

Figure 2.5. Localized and hybrid SON Architectures [18].

of cells and UE measurements. More advanced SON features provide dynamic LB between LTE network and different RATs such as between LTE and 3G/ HSPA.

Each eNodeB continuously monitors the cell load status and detects the overloaded cells. Activation of MLB functionality shifts the excessive load from overloaded cells to the less loaded neighboring cells automatically. This is achieved by changing virtual cell borders and triggering handover procedure for the users that are located at the cell-edge of the overloaded cells. Since less loaded cells have available resources to accommodate more users, this operation provides more efficient usage of radio resources, improves bandwidth efficiency of cell-edge users and reduces the number of unsatisfied users.

In connected mode LB, the eNodeBs know the QoS requirement and radio condition of each connected UE and the load state of other base stations. As a result, more accurate decisions can be made for LB. According to [1], MLB algorithms in connected mode should provide the following actions:

- Each eNB monitors the load in serving cell and exchange the load information with neighboring cells.
- Algorithm should evaluate the load information and determine if the serving cell

is overloaded or not.

- Algorithm modifies the HO parameters to satisfy the required HO triggering condition.

  Finally, some UEs at the cell border are handedover to less loaded cells, capacity of the system increases and human intervention in network management is avoided.

Connected mode MLB is analyzed for the cases between intra-frequency, inter-frequency and inter-RATs. In the intra-frequency case, HO operation is done between two LTE cells that use same carrier frequency. The source and the target cell share the same portions of the bandwidth so the cells create interference on each other. In the inter-frequency LB refers cases when UE moves between the cells which use different frequency carriers. The benefit is there is no mutual interference between cells and there is more degrees of freedom when selecting possible candidate UEs for LB. Finally, in inter-RAT LB, handover operation is forced between two different RATs such as 2G and 3G.

2.4.1. Intra-Frequency Mobility Load Balancing in LTE

In the scope of the thesis, we focus on connected mode MLB. In Figure 2.6 sequential flow of the intra-frequency MLB is illustrated as specified in the LTE standards. According to [19], the eNodeBs monitors the load of the cell and once a cell is detected to be overloaded, then load balancing functionality is activated. Before any actions, the overloaded cell needs available resource and load information of its neighbors, i.e. potential target cells. This information is transferred with resource status reporting procedure via X2 interface based on a client-server mechanism. The overloaded eNB sends 'Resource Status Request' message to request the load reports from its neighbors. Requested neighbors prepare 'Resource Status Response' or 'Resource Status Update' messages which consists cell identifiers, hardware load indicator information element (IE), transport network load IE, radio resource usage IE and composite available capacity (CAC) IE. Radio resource usage is the PRB usage separately for guaranteed bit rate and non-guaranteed bit rate users and separately for downlink and uplink. CAC of a cell is the amount of additional resources that can be accepted and signaled in

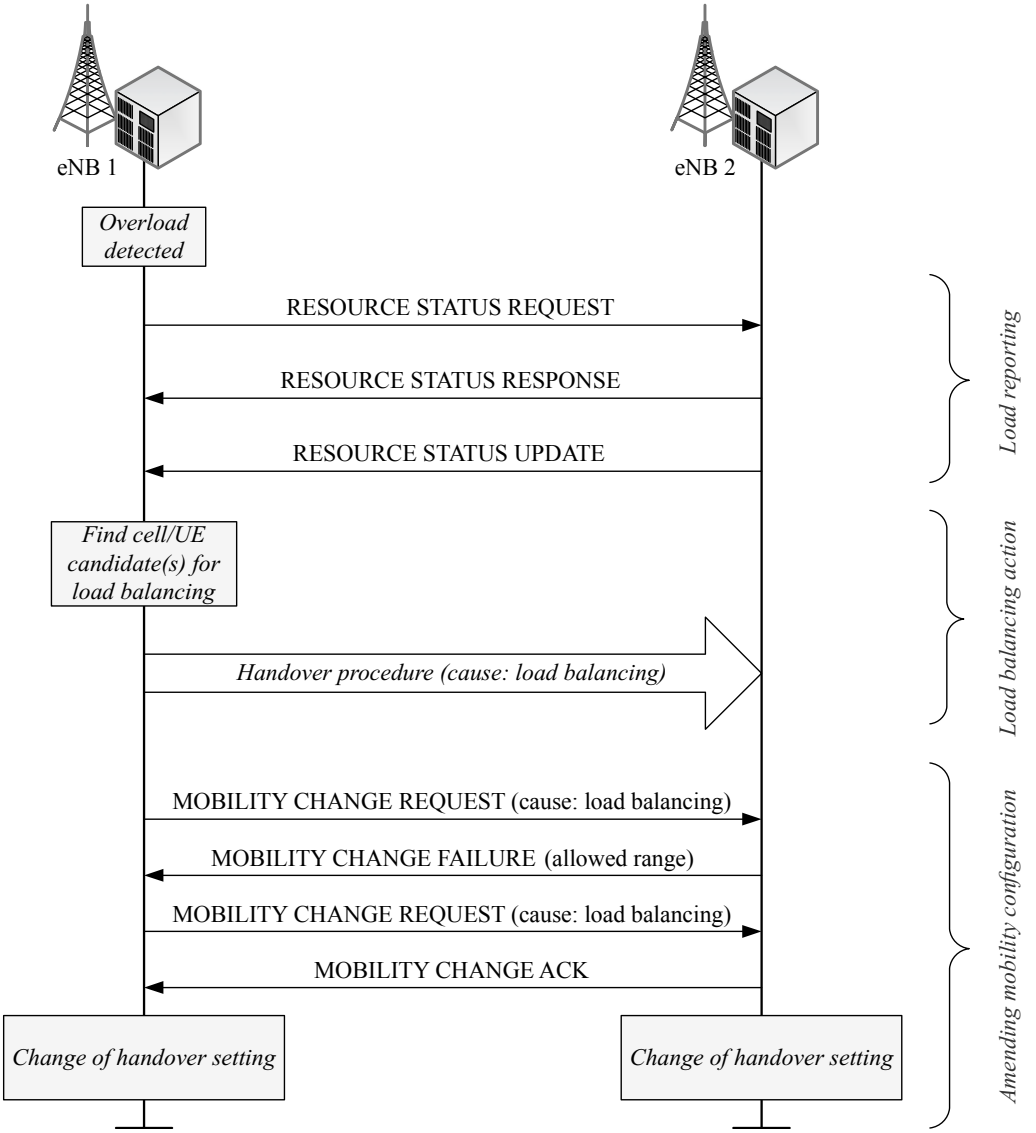

Figure 2.6. LB standardized solution [1].

percentage.

After having the necessary information related with the neighboring cells, the target cell is selected among all candidate neighboring cells. In LTE specifications, it is assumed that the connected UEs send measurement reports to the serving eNodeBs periodically. The measurement reports consists of reference signal received power (RSRP) and reference signal received quality (RSRQ) of each users measured from serving and

neighboring cells. The candidate users which are capable for handover are specified by using measurement reports. The target cell-user pair selection method differs according to the algorithm that is applied. After selection of target cell, HO parameters are modified to their possible new values. The HO parameters and conditions will be detailed in Section 2.4.3. In release 9, mobility change procedure is introduced. In mobility change procedure the cells that involved in HO procedure negotiate on new possible HO parameters. This negotiation guarantees that the UE handedover to neighboring cells will not be sent back due to radio conditions. If the proposed HO parameter adjustment is acceptable for the target eNB then 'Mobility Parameter Acknowledgement' message is sent, otherwise 'Mobility Parameter Failure' message is sent. After the negotiation, eNodeBs start handover procedure according to new parameter settings.

2.4.2. Load Calculation

In this section, the mathematical framework behind load calculation is presented as stated in [20]. In LTE, the load is defined as the ratio of used resources to all available resources in a given cell. Before the load metric is formulated, the instantaneous signal to interference and noise ratio (SINR) will be defined. Since the investigations about MLB are done under universal reuse factor, it is assumed that the total bandwidth is available by the users and bandwidth is not divided into sub-bands. That is the reason why the sub-band that the users assign is not considered while calculating SINR and related variables in [20]. The details about frequency reuse will be given in Section 3.2.1. It is also assumed that each UE measures the instantaneous signal strength from its serving cell and all neighboring cells through pilot detection and reports to the serving eNB. SINR measured on a single PRB of user u from serving cell c is defined as

$$SINR_u = \frac{P_c L_c(\overrightarrow{q_u})}{\sigma^2 + \sum_{z \neq c} \rho_z P_z L_z(\overrightarrow{q_u})} \tag{2.1}$$

where P_c and P_z are the transmit power from the serving cell c and neighboring cell z, $(\overrightarrow{q_u})$ is the position of user u relative to cell c, $L_c(\overrightarrow{q_u})$ and $L_z(\overrightarrow{q_u})$ are the position

dependent pathloss results from distance dependent pathloss, shadowing and angle dependent antenna patterns from the serving cell c and neighboring cell z, σ^2 is the thermal noise power and ρ_z is defined as the fraction of used PRBs in cell z. Given with $SINR_u$, the highest achievable bandwidth efficiency for user u per PRB is denoted as $R[SINR_u]$ and calculated by Shannon's spectral efficiency formula as in the following,

$$R[SINR_u] = \log_2(1 + SINR_u)(bits/s/Hz). \tag{2.2}$$

Shannon's formula gives an upper bound to the bandwidth efficiency and called as the Shannon bound. However, the Shannon bound is not practical, for a realistic approximation the measured $SINR_u$ should be mapped to the best modulation and coding scheme (MCS). Resulting achievable bandwidth efficiency for a single PRB is obtained from the look-up-table created according to link-level simulations.

Load of cell c is defined as

$$LOAD_c = \frac{\sum_{u \in \mathbf{U_c}} N_u}{N_{tot,c}} \tag{2.3}$$

where $\mathbf{U_c}$ is the set of CBR users connected to cell c, N_u is the actual number of PRBs scheduled for u and $N_{tot,c}$ is the total number of PRBs reserved for cell c. While calculating the load, one other important parameter is the value of QoS requirement of user u. The users demand different number of PRBs according to their QoS requirements. If service type of the user u is constant bit rate (CBR), then the number of PRBs that is required to serve user u is

$$\widehat{N_u} = \frac{D_u}{R[SINR_u](BW_{PRB})} \tag{2.4}$$

where D_u is the CBR requirement of user u and BW_{PRB} is the transmission bandwidth of a PRB which is 180 KHz in LTE system. $N_u = \widehat{N_u}$ only holds when the CBR requirement of user u is satisfied. However, in general some of the users are not satisfied and $N_u \leq \widehat{N_u}$. For the overloaded cells, the virtual load concept is introduced as the sum of the number required PRBs of all users u connected to the cell c and

given as in the following equation

$$\widehat{LOAD}_c = \frac{\sum_{u \in \mathbf{U_c}} \widehat{N_u}}{N_{tot}}. \tag{2.5}$$

If $\widehat{LOAD}_c \leq LOAD_{th}$, it means all the users meet with their CBR requirements, in other words all the users are satisfied. When the load exceeds a predefined threshold $LOAD_{th}$ that indicates overload condition and the overloaded cell becomes a source cell. Since virtual load can be greater than 1, virtual load is a better indication of overloaded condition rather than real load. In overloaded cells some users become unsatisfied and the number of unsatisfied users is calculated theoretically as in the following equation

$$Z_c = \sum_c \max \left(\sum_{u \in \mathbf{U_c}} |\mathbf{U_c}| * \left(1 - \frac{1}{\widehat{LOAD}_c} \right) \right). \tag{2.6}$$

Table 2.1. HO parameters.

HO Parameters	Meaning	Adjustments
F_s, F_n	Frequency-specific offset of source and neighboring cells respectively	Adjustable parameters for inter-frequency MLB
O_s, O_n	Cell-specific offset of source and neighboring cells respectively	Most common adjustable parameters
Off	Event based offset	Fixed value not adjustable
H	Event based hysteresis	Fixed value not adjustable
TTT	Time-to-Trigger	Adjustable based on user speed

2.4.3. Handover Procedure

According to [19] the conditions that trigger HO are mainly categorized into three event groups namely A3, A4 and A5 events. Table 2.1 and Table 2.2 summarize the HO parameters and the HO events with the parameters they adjust, respectively. In

general, HO procedure is modeled based on A3 event and the A3 event condition is

$$R_n + O_{n,s} + F_{s,n} > R_s + O_{s,n} + F_{s,n} + H \tag{2.7}$$

where R_n and R_s are the RSRP values from neighboring cell n and serving source cell s respectively in dBm. $O_{n,s}$ is the cell individual offset (CIO) of cell s with respect to cell n, $O_{s,n}$ is the CIO of cell n with respect to cell s and $F_{n,s}$ is the frequency specific offset (FSO) of cell s with respect to cell n, $F_{s,n}$ is the FSO of cell n with respect to cell s and H is the hysteresis. If the measured received signal strengths (RSRP or RSRQ) of serving and neighboring cell satisfy the A3 event HO condition in the period of Time-to-Trigger (TTT), HO procedure from serving cell to target neighbor cell is initiated. For intra-frequency case the FSO terms can be omitted and the HO condition given in Equation (2.7) becomes

$$R_n + O_{n,s} > R_s + O_{s,n} + H. \tag{2.8}$$

If we rewrite Equation 2.8, the following inequality is obtained.

$$R_n - R_s > O_{s,n} - O_{n,s} + H. \tag{2.9}$$

It is seen that decreasing $O_{s,n}$ or increasing $O_{n,s}$ makes the HO from cell s to the cell n easier, thereby reduces cell load. Load balancing is performed increasing $O_{n,s}$ in steps of Δ in the range of $[CIO_{min}, CIO_{max}]$. As in [22], $O_{s,n}$ and $O_{n,s}$ are kept in symmetric in order to prevent ping pong effect. Figure 2.7 shows an example of handover triggering by A3 event from source cell s to a neighboring cell n.

2.4.4. Literature Review

In recent years, MLB studies are very popular. In this section, some of the related works on MLB are reviewed. In [23], the aim of the study is to find the optimum CIO value which allows maximum number of users to make HO for LB purposes. During the algorithm the CIO value of the source cell is increased in constant step-size in

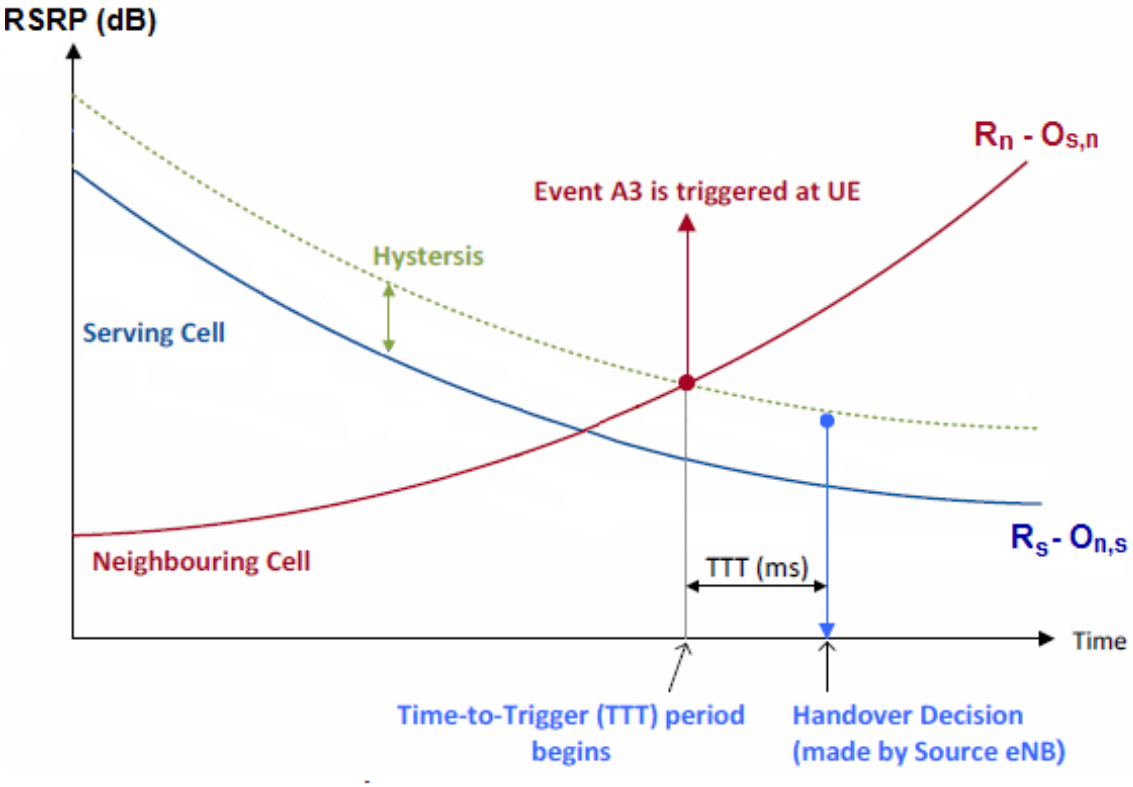

Figure 2.7. A3 event measurements.

Table 2.2. HO events and related parameters.

Events	Summary	Related Parameters
$A3$	RSRP from neighbor cell becomes better than RSRP from serving cell plus cell individual offset	$O_n, O_s, F_n, F_s, H, Off, TTT$
$A4$	RSRP from neighbor cell becomes better than a specified threshold	$O_n, O_s, F_n, F_s, H, Off, TTT$ threshold
$A5$	RSRP from neighbor cell becomes better than a specified threshold whereas RSRP from serving cell is worse than a threshold	$O_n, O_s, F_n, F_s, H, Off, TTT$ $threshold_1, threshold_2$

order to satisfy A3 event condition for cell edge users. A method for load estimation after handover would occur is proposed which is based on SINR prediction and user measurements.

Differently from [23], in [24] the CIO between neighboring cells is adjusted adaptively depending on the load difference. Using adaptive step size instead of constant step size decreases signalling overhead and increase efficiency of LB. For example, if the load difference between two neighbor eNodeBs is greater than a predefined threshold, the step size will be larger and the balance among cells is provided more quickly than using constant step-size. The drawback of the proposed technic is its computational complexity.

In [25], load state of a cell is divided into four regions. If the load state is in low loaded region energy saving functionality is activated. When the load state corresponds overload region, MLB functionality is triggered. The neighbor cell with the lowest load is assumed to the most prioritized target cell for HO operation. A utility function which based on the amount of CIO parameter that should be changed for HO and the load of target cell defined and the UE and neighboring cell pair that minimizes the utility function is selected for HO operation.

In [26] and [27] LB is investigated for heterogeneous services, i.e. best effort and CBR. The objective functions of the proposed algorithm are Jain's fairness index for CBR users and network wide utility function for BE users. After the UE-eNodeB pair which maximizes the objective functions is determined, HO operation is initiated as long as there is enough capacity in the target cell. According to the algorithm the users with higher QoS requirements should be guaranteed firstly. Therefore, the resources first allocated to the CBR UEs and then BE UEs. Although the results improve the performance for the overloaded cell, the handover parameter adjustment is not implemented. In [28], the latter work of the authors of [26] and [27], also considers the load of network. The aim is to balance the load distribution among neighboring cells as much as possible while increasing the network average load as little as possible.

All the aforementioned solutions shift the excessive load of the overloaded cell only to the adjacent neighbors of overloaded cell. In some situations one of the less loaded adjacent neighbors can be selected as a target cell by more than one overloaded cell and it causes a risk of creating another overloaded cell. The method proposed in [29]

defines the adjacent neighbors as first layer neighbors and the neighbors of adjacent neighbors as second layer neighbors. The overloaded cells take into account the load state of both first and second layer neighbors while it is selecting the target cell while selecting the target cell. Although consideration of second layer neighborhood gives better performance than conventional MLB method, it may not be very preferable for practical purposes since it requires additional information. In [22], before HO initiation the load that will be created in the possible target cell is estimated. If the amount of available capacity in the target cell is not enough to serve the handedover UE, the target cell shifted some of its connected users to its adjacent neighboring cells. This method called as 'secondary MLB' or 'neighborhood MLB'. Besides the disributed solutions, the central MLB solution is presented in [30]. According to the model, there is a central server that collects information about the PRB utilization of all eNodeBs. The central server compares PRB utilization status of each eNodeBs with a predefined threshold and detects the overloaded cells. On the other hand, in [31] a hybrid model is presented. Load status information is exchanged between eNBs via X2 interface as in distributed solution and monitored by a high level element, i.e. OAM entity as in central solution.

When different SON functionalities try to optimize the same HO parameters in the opposite direction a conflict may happen. MRO is one of the self optimization functions which aims to minimize the radio link failures (RLFs) and ping-pong HO by optimizing HO parameters H, CIO and TTT. Although the two functions, MLB and MRO, operate independently with each other, there is a close correlation between them. For example, when MLB adjust a HO parameter for LB purposes, same handover parameter can be changed back by MRO functionality to prevent a possible handover problem that causes RLF as stated in [1]. The conflict may lead a closed loop and decrease the network performance. In [32], a method is proposed to solve the conflict problem between MLB and MRO. Principle of the proposed method is to avoid RLF problems, therefore the operation of MLB is restricted. According to the scheme, MLB can modify the CIO parameter only in an allowed range. In order to identify the upper and lower limits of the allowed range, source cell requests current CIO, hysteresis and the maximum CIO value that causes too late handover, i.e. CIO_{late}, from target

cell. Source cell measures the minimum CIO value that causes too early handover, i.e. CIO_{early}, and the upper and lower limit of allowed range is identified as CIO_{early} and CIO_{late} respectively. A further research, [33], also considers the speed of users while defining the allowed CIO range. In the proposed scheme, different TTT values are set for different speed of users. For example, as the speed of a UE is getting higher, TTT value becomes smaller to react the fast changing network conditions quickly. Adaptive TTT values also change the minimum CIO value that causes too early handover and the maximum CIO value that causes too late handover hence the allowed range is affected from TTT parameter.

LB functionality is also investigated in LTE-Advanced (LTE-A) cellular networks. Heterogeneous network (Het-Net) is one of the feature of LTE-A which has a topology of mixed macro-cell and low power nodes (LPNs), i.e. pico cells, micro cells as detailed in [34]. In Het-Nets, the UEs tend to connect to the macro-cells since macro cells serve higher transmit power. As a result, only a small number of UEs connect to the LPNs and the load becomes imbalanced among the macro-cells and LPNs. In [35] the load imbalance problem is solved with range extension of LPNs. The methodology is based on adding offset to LPNs to maximize their coverage without changing their transmit power so that UEs are handedover from macro-cells to smaller cells. The other study [36] investigates the disadvantages and advantages of handover parameter control and cell coverage control. In CCC, coverage is adjusted by changing antenna tilt or pilot power. This method achieves higher offloading performance than HPC whereas it creates interference among neighbor cells. In the proposed algorithm, when an eNB is detected as overloaded, first the offloading effect achieved by HPC is estimated. If the overload situation is resolved then the algorithm selects HPC, otherwise it applies CCC.

Although there have been a significant number of studies investigating MLB, all of them investigate MLB under universal reuse factor, i.e. reuse-1. On the other hand, only a very limited number of research consider LB under ICI mitigation techniques. For example, in [37], investigate LB in a multi-cell FFR network and in [38], Son's work [37] is extended by admitting users with heterogeneous service requirements. In

each study an objective function is defined and the user-cell pair that maximizes the objective function is selected as candidates. Due to the fact that these works do not consider LB in the scope of MLB, handover operation is not modeled with handover parameter adjustment. Instead, LB operation is basically executed by assigning the selected user to the selected target cell. Additionally, there has been no research which investigate MLB and even LB in SFR network. It can be concluded that there is a lack of research which considers MLB and ICIC jointly.

3. RADIO RESOURCE MANAGEMENT (RRM)

Radio resource management (RRM) comprises the techniques which are used to utilize the radio resources as effective as possible. In LTE, RRM controls the parameters like transmit power, selected modulation scheme, handover parameters, error control coding method and channel allocation. These parameters are optimized in order to design a system that ensures QoS requirements of services, maximum coverage, high spectral efficiency and an acceptable level of fairness among the users while allocating radio resources. Knowledge of radio link quality of users is a very useful tool while trying to achieve the system requirements. Additionally, the link quality of a connected user may fluctuate due to the changing network conditions i.e. path loss, multi-path propagation, shadowing, interference created by neighboring cells and noise level. Adaptation to the changing environment becomes very crucial and it is done by link adaptation.

Link adaptation (LA) is a process that compensates the variations in the instantaneous channel conditions with the help of adaptive modulation and coding scheme (AMC) stated in [39]. AMC tries to match the achieved information data rate for each user to the variations in received signal quality by adjusting modulation and coding scheme according to channel conditions although the power of the transmitted signal is unchanged. The method suggests to use more robust and low order modulation schemes (e.g. QPSK) for the users locate far from cell center or has low SINR and use higher order modulation schemes (e.g. 64 QAM) when the SINR is sufficiently high in data transmission. As a result, the bit error rate can be kept under an acceptable level.

However, in downlink transmissions, the eNodeB does not directly know the actual measured SINR value of an UE, instead the eNodeB receives channel quality indicator (CQI) information form terminals. Once a UE measures the SINR value, it calculates the CQI based on the subcarrier SINR and the target BLER, then the UE reports the CQI value to the served eNodeB as an uplink feedback [2]. For a target

BLER 10%, SINR to CQI mapping is approximated in Figure 3.1. Table 3.1 contains the appropriate modulation scheme, channel coding rate and achievable efficiency corresponding to the CQI value and according to the table, it is observed that higher CQI value indicates better channel quality and higher data transmission rate [12].

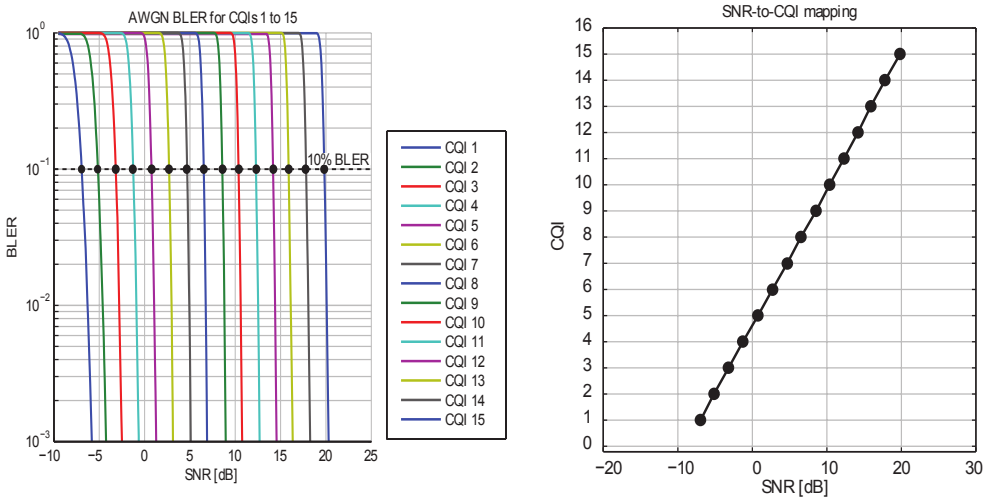

(a) CQI BLER curves

(b) SINR to CQI mapping obtained from 10% BLER curves

Figure 3.1. SINR to CQI mapping [13].

Main functionalities of RRM are provided scheduling and frequency planning schemes which are developed interference management. In this chapter, scheduling and frequency planning schemes are detailed.

3.1. Scheduling

Scheduling is the distribution of time-frequency resources between UEs and it is carried out by a scheduler. The downlink physical resource is represented as a time-frequency resource grid consists of multiple PRBs. A PRB is the smallest unit that can be scheduled to a UE in a sub-frame and consists of 12 adjacent sub-carriers and has a bandwidth of 180 KHz as previously mentioned in Section 2.2.2. In LTE, a sub-frame corresponds to transmission time interval (TTI) which is 1ms. Since one aspect of this study is to compare MLB performance of different scheduling methods, this section will present a brief overview about round-robin, best CQI and proportional fair schedulers.

Table 3.1. 4-bit CQI table.

CQI index	Modulation	Coding rate	Efficiency [bits/s/Hz]
0		Out of range	
1	$QPSK$	78/1024	0.1523
2	$QPSK$	120/1024	0.2344
3	$QPSK$	193/1024	0.3770
4	$QPSK$	308/1024	0.6016
5	$QPSK$	449/1024	0.8770
6	$QPSK$	602/1024	1.1758
7	16QAM	378/1024	1.4766
8	16QAM	490/1024	1.9141
9	16QAM	616/1024	2.4063
10	64QAM	466/1024	2.7305
11	64QAM	567/1024	3.3223
12	64QAM	666/1024	3.9023
13	64QAM	772/1024	4.5234
14	64QAM	873/1024	5.1152
15	64QAM	948/1024	5.5547

3.1.1. Round-Robin Scheduling

Round-Robin scheduling assigns resources to the users cyclically without taking the instantaneous channel conditions into account. Main advantage of round-robin scheduler is the guaranty of great fairness among the users in radio resource assignment. Furthermore, it is very easy to implement. On the other hand, it offers poor performance in terms of system throughput since the CQI feedbacks are not considered.

There are two types of implementation of round-robin scheduling, namely the time domain round-robin and time and frequency domain round-robin. In TDRR a single user is assigned the whole spectrum in a specific time period and the next user is scheduled in the next time period. In TFDRR multiple numbers of users are served

in the same time period. The steps of round-robin scheduling algorithm is illustrated in the flow chart given in Figure 3.2.

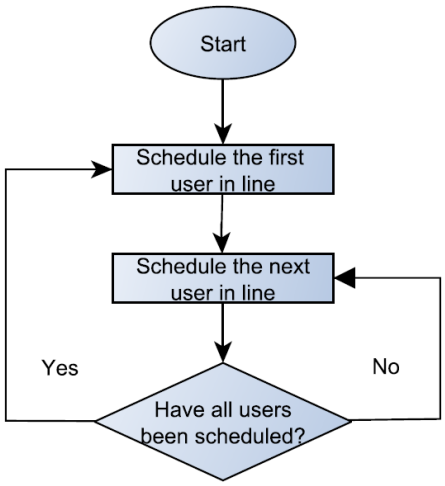

Figure 3.2. Flow chart of round-robin scheduling algorithm [40].

3.1.2. Best-CQI Scheduling

The best-CQI scheduler allocates the resources to the user with the best radio link conditions as stated in [41]. The UEs measure the received SINR and based on measured SINR they send CQI feedbacks serving eNodeBs periodically. When best-CQI scheduling is applied, the UE with good channel quality, i.e. SINR, enhances its peak data performance and the total throughput of the cell is maximized. However, the users that locate far from the serving eNodeB, i.e. cell-edge users, become unlikely to be scheduled since they have relatively less SINR.

3.1.3. Proportional Fair Scheduling

Proportional fair scheduler aims to provide an acceptable throughput level while improving fairness among users. Main goal of the scheduling algorithm is to find a good trade-off between system throughput and fairness. It takes the channel conditions of the users into account. In the beginning, the eNodeB schedules the users which have the higher CQI and in the subsequent slots the users are scheduled in cyclic order.

Figure 3.3 depicts a possible implementation of a proportional fair scheduler. Authors

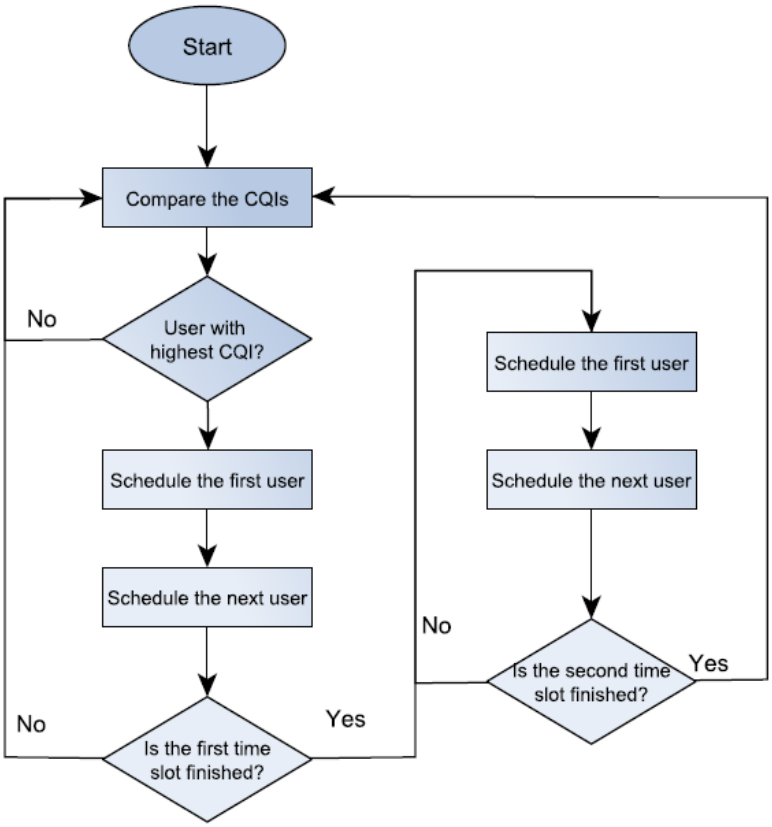

Figure 3.3. Flow chart of proportional fair scheduling algorithm [41].

of [42] and [43] present a comparative work that evaluates the throughput and fairness conditions for the scheduler types stated above.

3.2. Static Inter-Cell Interference Coordination Approaches

In LTE, downlink transmission scheme is based on OFDMA. OFDMA supports intra-cell orthogonality, in other words there is no intra-cell interference created on connected users. However, when the same portion of the system bandwidth is used different neighboring cells, there exists inter-cell interference (ICI). ICI lowers the overall capacity of cell. Especially, the cell-edge users suffer from strong ICI and can achieve very low transmission rate since their measured SINR becomes very low with increasing interference. To solve the interference problem, there have been suggested various ICI mitigation methods. Reusing the frequencies in a designated region is one of the common ICI mitigation methods in the scope of static ICIC approaches. In this section,

firstly frequency reuse concept is summarized with its trade-offs and then more advance reuse method namely fractional frequency reuse (FFR) is detailed by explaining its two different deployments.

3.2.1. Reuse Factor

Frequency reuse suggests to reuse the same channel/frequency in different cells which are far from each other. Allocation of the same group of resources to the different cells for completely different transmissions improves spectral efficiency and capacity. Performance of frequency reuse method depends on frequency reuse factor. Frequency reuse factor is a parameter that indicates the rate of usage of the same frequency in the network. Frequency reuse factor 1 corresponds the universal reuse scheme and when universal reuse scheme is applied, total bandwidth is available for all cells. Universal reuse scheme provides high spectrum efficiency, however cell edge users suffers from inter-cell interference since adjacent cells use the same frequency bands. In order to solve the interference problem, the common values frequency reuse factor 3, 4, 7, 9 or 12 can be used. For example, when frequency reuse factor is chosen as 3, the total bandwidth is divided into three sub-bands and each sub-band is assigned to three different neighboring cells one by one. Therefore, interference experienced by the cell-edge users is remarkably reduced. On the other hand, the resource allocated to each individual cell becomes one third of total bandwidth and the limited usage of resources is expected to degrade the spectrum efficiency and the cell throughput. This situation points out the trade-off between network capacity and the amount of inter cell interference mitigation. Figure 3.4 illustrates the resource allocation scheme for reuse factor 3.

3.2.2. Fractional Frequency Reuse

The FFR scheme was firstly proposed for GSM networks, then standardized for LTE. FFR scheme divides the cell area into two regions according to the distance to the base station [45]: exterior region which spans cell-edge users and interior region which spans the users that locate close to the serving eNodeB. The bandwidth assigned

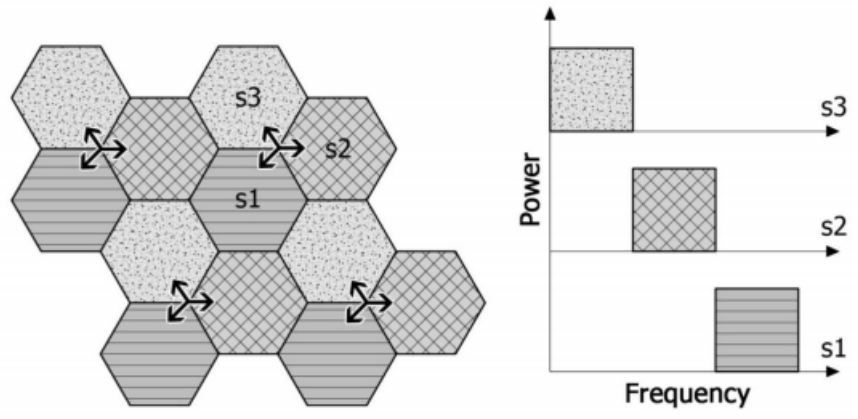

Figure 3.4. Conventional frequency planning with reuse factor 3 [44].

to each cell is partitioned into two subset called as inner band and outer band. Inner band is allocated for the users that locate in the interior region, while latter is allocated for the users that locate in the exterior region. As a result, the interference created on cell-edge users from both the interior and exterior regions of adjacent cells is reduced.

In practice, user to sub-band allocation is based on time averaged SINR calculations. The users with having SINR value greater than a threshold are assigned to the inner band and others are assigned to the outer band. In reality, the boundary between inner and outer band is irregular due to shadowing and fading whereas for the ease of presentation the boundary can be depicted with straight lines as the inner circle shown Figure 3.5. Since the time averaged SINR is a good indicator about the distance between the base station and the users, change in the SINR threshold results with the change in the radius of interior circle and the number of users assigned to inner and outer bands.

According to the [46], there are two main types of FFR deployments: strict FFR and soft frequency reuse (SFR).

(i) *Strict Fractional Frequency Reuse:* In strict FFR, the interior users do not share any bandwidth (sub-carriers) with cell edge users. On the other hand, the interior users of all cells use a common sub-band of frequencies as illustrated in Figure 3.5(a) and the rest of the bandwidth is partitioned for cell-edge users with relying

a reuse factor of N=3. In total, strict FFR requires N+1 mutually orthogonal sub-bands. Orthogonality reduces the interference on cell-edge and interior users at the expense of spectral efficiency.

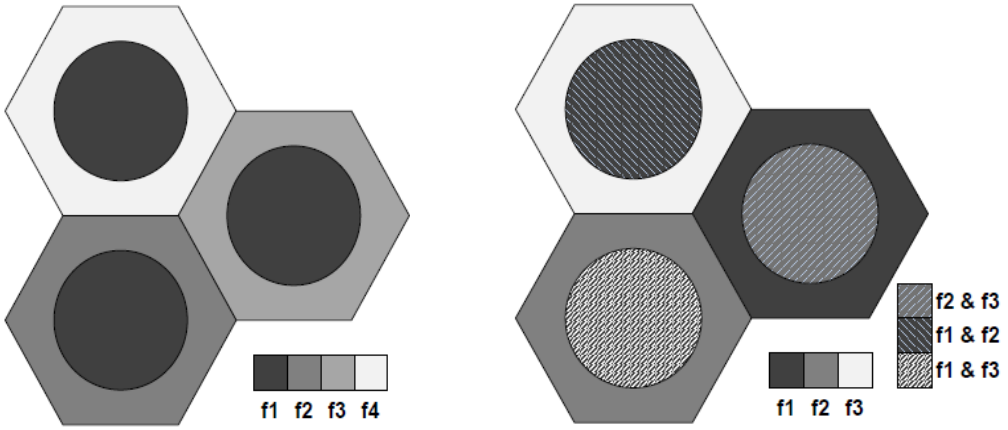

(a) FFR (b) SFR

Figure 3.5. FFR and SFR deployments with N = 3 cell-edge reuse factor [46].

The interior radius R_{int} can indicate the regional boundaries of inner and outer bands. If we assume that N_{int} is the number of PRBs allocated to inner band, the number of PRBs allocated to outer band N_{ext} is calculated as

$$N_{out} = \frac{N_{tot} - N_{int}}{3}. \tag{3.1}$$

Strict FFR is simply referred as FFR for the remainder of the thesis.

(ii) *Soft Frequency Reuse:* In SFR, the cell-edge region applies frequency reuse factor N=3 and the edge users of adjacent neighboring cells use mutually orthogonal bands as in the case of strict FFR. In the interior region, the users are allowed to share the cell-edge sub-bands of the adjacent neighboring cells. In total, SFR requires N mutually orthogonal sub-bands, therefore the bandwidth is utilized more effectively compared to strict FFR. However, cell-edge users suffer from interference created by the interior users of neighboring cells. In order to mitigate the interference, the downlink transmission power for interior users is reduced. Level of the reduction is controlled by a power control factor. Generally used power control values are 2 or 4 which correspond to cell-edge user gains of 3 dB

and 6 dB, based on heuristic results in [47].

In Figure 3.5(b) frequency planning scheme for SFR is depicted. In SFR, the number of PRBs allocated for exterior users is calculated as

$$N_{out} = \min\left(\frac{N_{tot}}{3}, N_{tot} - N_{int}\right). \tag{3.2}$$

4. INTER-CELL INTERFERENCE COORDINATION AWARE MOBILITY LOAD BALANCING

This section summarizes the framework of the considered MLB solution which is executed in a static ICIC aware manner. The functionalities related with MLB are implemented in eNodeBs individually in as in distributed architecture. In this study, MLB process is described with two phases, i.e. monitoring and balancing.

In MLB, balancing refers to achieve a more balanced load distribution between neighboring cells which defines inter-cell MLB. Inter-cell MLB framework can be summarized as follows. According to the 3GPP standardization [19], each eNodeB monitors and evaluates the load state of the controlled cell in monitoring phase. If the load state of the controlled cell is greater than a predefined threshold $LOAD_{th}$, the cell is assumed to be overloaded. First step of the balancing phase is the load state exchange operation between overloaded eNodeB and its neighbors. The overloaded cell request load state information from neighboring eNodeBs and send its own load state to them. The overloaded cell uses the knowledge of load information of neighboring cells in order to be able to select the appropriate target eNodeB (TeNB). The TeNB is chosen from the adjacent neighboring eNodeBs which is willing to accept the excessive load of overloaded cell. TeNB selection methodology can differ according to the implemented algorithm. After TeNB is determined, the standardized mobility parameters are adjusted to direct some of the cell-edge users to the TeNB.

In addition to inter-cell MLB, for some frequency planning schemes, i.e. strict FFR and SFR, which divides the cell into two geographical regions and assign different sub-bands to these regions, it is needed to apply an additional balancing methodology which balance the load between two geographical regions/bands. Intra-cell LB is a method that avoids load imbalance between inner and outer bands of a cell with execution of intra-cell HO. Intra-cell HO is just the mechanism that triggers to change the band currently being used. Comparing to inter-cell HO, intra-cell HO brings low

system overhead. Thus the periodicity of inter-cell HO is larger than inter-cell HO. In the following sections, monitoring and balancing phases will be detailed.

4.1. Monitoring Phase

In the monitoring phase, the eNodeB monitors the virtual load of the controlled cell. In Section 2.4.2, the virtual load of cell c is defined as the ratio of sum of the number of PRBs that is required to satisfy QoS requirement of connected UEs to the total number of PRBs available in cell c. The total number of PRBs available to each cell depends on sub-band assignment. Sub-band assignment is determined according to the applied frequency-planning scheme. Reuse-1, reuse-3, strict FFR and SFR are the frequency-planning schemes which we consider in this thesis. Therefore, the virtual load calculation implementation is now detailed considering the sub-band assignment strategy.

- *Virtual Load Calculation Implementation:* Frequency reuse methods reuse the channels by dividing the allocated band into sub-bands in order to reduce the ICI and improve spectral efficiency. As detailed in Section 3.2, frequency reuse with factor N, divides the total bandwidth into N sub-bands and each sub-band is allocated to N different neighboring cells. Strict FFR and SFR also apply resource partitioning and the cell-edge users of a cell are assigned with a sub-band group different from both interior users of same certain cell and the cell-edge users of different neighboring cells.

  First of all, the SINR expression is reformulated considering the sub-bands and according to the model we simulated. Our model only considers the path loss and small scale fading effects and we ignore shadowing and fast fading effects for simplicity. The received SINR for user u from base station c on PRB l in band w can be written as:

$$SINR^w_{clu} = \frac{P^w_{cl} h^w_{clu} G_{cu}}{\sigma^2 + \sum_{z \in Q^w_c, z \neq c} P^w_{zl} h^w_{zlu} G_{zu}} \tag{4.1}$$

  where P^w_{cl} and P^w_{zl} are the downlink transmit powers of serving cell c and inter-

fering cells on PRB l in band w, respectively. h^w_{clu} denotes the channel fading coefficient between cell c and user u on PRB l in band w, which is assumed to be exponentially distributed. The path loss between the base station and the user is calculated as $G_{cu} = \|\mathbf{c} - \mathbf{u}\|^{-\alpha}$ where $\mathbf{c}$ and $\mathbf{u}$ denote the coordinates of the base station c and user u and α is the pathloss exponent. Q^w_c is the set of base stations that use band w as cell c therefore interfering with user u. For reuse-1, reuse-3 and FFR P^w_{cl} is fixed for all base stations. On the other hand, in the case of SFR a power control factor is introduced to create two different power classes. In this study, power control factor values are 1 and 4, which corresponds to gain of 0 and 6 dB gain for cell edge users.

Expression in Equation 4.1 is matched with appropriate CQI index value. Given CQI index value, the instantaneous achievable bandwidth efficiency on PRB l of user u from base station c is obtained according to CQI mapping table given in Table 3.1 and denoted as $R\,[SINR^w_{clu}]$. The average bandwidth efficiency is the expectation of the instantaneous bandwidth efficiency among all PRBs assigned to band w and calculated as

$$R\,[SINR^w_{cu}] = \frac{1}{|\mathbf{S^w_c}|} \sum_{l \in S^w_c} R\,[SINR^w_{clu}] \tag{4.2}$$

where where $\mathbf{S^w_c}$ is the set of PRB in cell c in band w. The virtual load of the band w of cell c is formulated as

$$\widehat{LOAD}^w_c = \frac{\sum_{u \in \mathbf{U^w_c}} \widehat{N^w_{c,u}}}{N^w_{tot,c}} \tag{4.3}$$

where $\mathbf{U^w_c}$ is the set of users connected to cell c assigned in band w, $\widehat{N^w_{c,u}}$ is the required PRBs to meet CBR requirement of user u of cell c in band w and $N^w_{tot,c}$ the total number of PRBs available for CBR users allocated for band w of cell c. In reuse-1 $N^w_{tot,c}$ corresponds to the total bandwidth of the system. On the other hand, with the reuse factor of N, $N^w_{tot,c}$ corresponds to the one N'th of the total bandwidth. For example, in reuse-3 the $N^w_{tot,c}$ is one third of the number of total PRBs. Given the average bandwidth efficiency, the number of PRBs required to

serve user u from cell c in band w to meet the CBR requirement is calculated by

$$\widehat{N_{c,u}^{w}} = \frac{D_u}{R\left[SINR_{cu}^{w}\right](BW_{PRB})}. \tag{4.4}$$

Total virtual load of cell c becomes

$$\widehat{LOAD}_c = \frac{\sum_{w \in \mathbf{W}} \sum_{u \in \mathbf{U_c^w}} \widehat{N_{c,u}^{w}}}{N_{tot,c}} \tag{4.5}$$

where $\mathbf{W}$ the set of all bands in a cell. In the cases of SFR and FFR, $\mathbf{W}$ consists of the inner and the outer band and the total load of the cell c is equal to the sum of the total number of required PRBs for inner and outer band divided by $N_{tot,c}$.

The virtual load is compared with $LOAD_{th}$ which is assumed 95% of the PRBs allocated to cell c, if virtual load exceeds $LOAD_{th}$ then load balancing phase begins with exchange of load status information between neighboring eNodeBs.

4.2. Balancing Phase

In our algorithm, in the cases of reuse-1 and reuse-3, MLB implies inter-cell MLB and in the cases of FFR and SFR, the intra-cell LB mechanism is included in MLB functionality together with inter-cell MLB. Since the intra-cell LB has lower system overhead the execution period kept shorter compared to inter-cell MLB.

4.2.1. Inter-Cell Balancing

In inter-cell balancing, aim is to balance the load between neighboring cells directing the cell-edge UEs of each the overloaded cell by adjusting CIO parameter under the constraint that the neighborhood cells do not get overloaded due to new incoming UEs. Once a cell is detected as in overloaded state, it is named as a source eNodeB (SeNB). In inter-cell balancing phase, the SeNB is expected to execute the five main actions listed in the following list:

(i) Create the list of candidate TeNBs for HO.

(ii) Create the list of UEs which are capable for HO, i.e. candidate UE list.

(iii) Decrease the current CIO value between SeNB and candidate TeNB to a temporary CIO value and determine the UEs which satisfy HO condition if the current CIO value is changed with temporary CIO value.

(iv) Estimate the measured SINR and the load created in potential TeNB after HO operation of user u

(v) If there is enough resource in the TeNB to serve the handedover UE, update current CIO value to the temporary CIO value.

In the load information exchange procedure SeNB collects the virtual load information of all adjacent neighboring cells. A threshold which determines a load limitation for HOs operation of users is defined and denoted as $LOAD_{th,HO}$. If the load state of cell c exceeds $LOAD_{th,HO}$ than HO requests to cell c are not accepted by the call admission control mechanism. The candidate TeNBs for HO are the eNodeBs with load state less than $LOAD_{th,HO}$. In the first step, the SeNB determines the candidate TeNBs, sorts them in descending order and creates the list of candidate TeNBs. In the second step, the SeNB determines the users which are capable of HO. The users that locates on the cell-edge are able to HO to the potential TeNBs. Since SINR is a good indicator about the distance between SeNB and connected users, the users which have bad radio link conditions are assumed to be cell-edge users.

After the candidate TeNBs and users lists are created, the SeNB chooses the first entry from the candidate TeNB list, considers it as temporary TeNB, i.e. $TeNB_{temp}$ and decrease the temporary CIO value of SeNB respect to $TeNB_{temp}$, i.e. $O_{TeNB_{temp},SeNB}$, in steps of Δ from its current value until the handover condition given in Equation 2.9 is satisfied for any UE from UE list. In the implementation Δ is assumed to be 1 dB and the lower limit of CIO is assumed to be -5 dB. The idea behind the adjustment of temporary CIO is to predict the behavior of the system if the virtual cell border of the SeNB is changed due to the change of the current CIO value. Once the handover condition given in Equation 2.9 is satisfied for any user from the candidate UE list, the SeNB need to estimate two metrics in order not to be rejected by the call admission

control mechanism of TeNB. The metrics are the load created at TeNB after HO operation and the SINR with the TeNB. The load estimation will be detailed through the section. For user u the estimated load created in TeNB is denoted as $\widehat{LOAD}^{est}_{u,TeNB}$. If the TeNB has enough resources to serve the UE u with its CBR requirement as in the following equation

$$LOAD_{th,HO} - \widehat{LOAD}_{TeNB} > \widehat{LOAD}^{est}_{u,TeNB} \tag{4.6}$$

where $\widehat{LOAD}_{TeNB}$ is the virtual load state of the TeNB and if averaged SINR measured by UE u with the TeNB is greater then $SINR_{th,min}$ where $SINR_{th,min}$ is the minimum SINR value that should be satisfied in order not to cause an RLF, the current CIO value is updated to the temporary CIO value. Otherwise, the algorithm chooses the next cell from the candidate TeNB list. The process of selecting the next cell from potential TeNB list continues as long as CIO values are in the allowed range of $[CIO_{min}, CIO_{max}]$ and there are more potential cells in candidate TeNB lists which are able to accommodate additional load.

Up to now it is assumed that only the adjacent neighbors of the overloaded cell are involved in the MLB operation. In some cases, the load states of all cells in candidate cell list reach the value of $LOAD_{th,HO}$, in other words the adjacent neighbors do not have available capacity to accommodate additional load. In order to create extra capacity in the adjacent neighbors, non-adjacent neighbors can be involved into the LB operation. For the ease of presentation, we call the method that considers only adjacent neighbors as MLB 1 and the method that considers non-adjacent neighbors of overloaded cell as MLB 2.

In the next two items, we emphasize the details of estimation of created load on the neighboring eNodeB and MLB 2.

(i) *Estimation of SINR Load Created on Neighboring cell eNodeBs:* When a UE is handedover from one cell to another, the received SINR and the load created to support the service requirements will be different than its previously served

cell. The load transferred during HO operation should not exceed the available capacity in selected neighboring cell otherwise the call admission control mechanism of the TeNB rejects the HO requests. If the HO request is repeated, it causes significant signalling overhead. Additionally, the SINR with TeNB should be greater than $SINR_{th,min}$ to avoid RLFs. In order to avoid signalling overhead and RLF, SeNB should estimate the SINR with TeNB and load created in TeNB before sending HO request.

Assuming that UE u in band w is expected to satisfy the A3 event HO condition with the decreased temporary CIO value is determined, SeNB estimates the SINR with TeNB as in the following

$$SINR^{est}_{TeNB,u} = \frac{R_{TeNB}}{\sigma^2 + \sum_{z \in Z^{w_T}_{TeNB}, z \neq TeNB} R_z} \tag{4.7}$$

where w_T is the band which is assigned to TeNB, R_{TeNB} is the RSRP measured from TeNB R_z is the RSRP measured from interfering cell. $Z^{w_T}_{TeNB}$ is the set of cells which use same sub-band with TeNB and therefore will interfere UE u after HO operation where w_T is the band that outer band of target cell is assigned. In this approach, it is assumed that all PRBs which are assigned to UE u after HO operation will measure a unique SINR value. $SINR^{est}_{TeNB,u}$ is mapped to best MCS as stated in Section load calculation and we can estimate the achievable bandwidth efficiency $R\left[SINR^{est}_{TeNB,u}\right]$. Then the number of PRBs that is needed to fulfil the service requirement of UE u calculated as

$$\widehat{N^{w_T}_{TeNB,u}} = \frac{D_u}{R\left[SINR^{est}_{TeNB,u}\right](BW_{PRB})}. \tag{4.8}$$

Finally the load created at TeNB is

$$\widehat{LOAD}^{est}_{u,TeNB} = \frac{\widehat{N^{w_T}_{TeNB,u}}}{N_{tot,TeNB}} \tag{4.9}$$

where $N^{w_T}_{tot,TeNB}$ is the number of total available PRBs for CBR users in cell c allocated for band w_T.

(ii) *Mobility Load Balancing with Non-Adjacent Neighbors:* When there is no available capacity in the adjacent neighbors of SeNB, the adjacent neighbors are requested to direct some of load to non-adjacent neighbors to create additional required capacity and we referred this procedure as MLB 2. In our approach, it is inspired from the method given in [29] while choosing the possible TeNB. Each adjacent neighbor of overloaded cell collects the load state of its neighbors and takes the average to create the environment load state information. After calculation of the environment state, the adjacent neighbor i creates its overall load state as in the following expression

$$\widehat{LOAD}_{over,i} = \mu \widehat{LOAD}_i + (1-\mu)\widehat{LOAD}_{env,i} \tag{4.10}$$

where μ is a measure of influence of virtual load state of cell i to the overall load state and it is chosen as 0.8 in the implementation. $\widehat{LOAD}_{env}$ is the environment state and it is calculated as

$$\widehat{LOAD}_{env,i} = \frac{1}{|\mathbf{K}|} \sum_{j \in \mathbf{K}} \widehat{LOAD}_{ij} \tag{4.11}$$

where $\mathbf{K}$ is the number of adjacent neighbors and $\widehat{LOAD}_{ij}$ is the load state of adjacent neighbors of cell i. When the SeNB receives overall state information from its adjacent neighbors, SeNB sorts the adjacent neighbors according to their overall load state information in descending order. SeNB begins from the first entry of the list assumes the first entry as a possible TeNB. SeNB requests from possible TeNB to shift some of its load to its neighbor cells. The inter-balancing phase is activated for the possible TeNB although it is not overloaded. All in all the boundary UEs of the possible TeNB is forced to make HO to the non-adjacent neighbors of SeNB and the additional capacity is created at the possible TeNB for SeNB. Finally, possible TeNB becomes the actual TeNB and inter-cell LB is initiated between the overloaded cell and its actual TeNB.

4.2.2. Intra-Cell Balancing

In the cases of strict FFR and SFR, intra-cell LB is executed in addition to inter-cell MLB. As explained before, intra-cell LB aims to achieve balanced load distribution between inner and outer bands/regions. In general, the outer band tends to have greater virtual load than the inner band, since the number of PRBs reserved for the exterior region, i.e. N_{ext} is less than the number of PRBs reserved for the interior region, i.e. N_{int}. On the other hand, the exterior users requires more number of PRBs than the interior users to satisfy the same CBR requirement due to low SINR they measure.

The boundary between the interior and exterior regions is determined by the radius of the interior region of the cell R_{int}. In our approach, intra-cell LB is provided by the intra-cell HO mechanism which is triggered by modifying the value of R_{int}. Changing the band that is currently being occupied refers to intra-cell HO. For example, when the load of the outer band is higher than the load of the inner band, R_{int} is increased to transfer some users from the outer band to the inner band. The gain of intra-cell HO is measured by the intra-cell LB index. Intra-cell LB index of the system is formulated in [38] and given as

$$J_{intra}(x) = \frac{\sum_{c \in \mathbf{C}} (LOAD_c^w - LOAD_c^{\overline{w}})^2}{|\mathbf{C}|} \tag{4.12}$$

where $\mathbf{C}$ is the number of cells in the network, $\overline{w}$ is the opposite band to band w. The load balance index takes a value in the interval $[0, 1]$. The smaller intra-cell LB index means the difference between the loads of opposite regions is less. Before HO $J_{intra}(x)$ is assumed to be $J_{intra}^{before}(x)$.

After intra-cell HO, intra-cell LB index is expected to become

$$J_{intra}^{after}(x) = \frac{\sum_{i \in \mathbf{C}, i \neq c} (LOAD_i^w - LOAD_i^{\overline{w}})^2 + \left[(LOAD_c^w - \mathbf{x}) - (LOAD_c^{\overline{w}} + \mathbf{y}) \right]^2}{|\mathbf{C}|} \tag{4.13}$$

where $\mathbf{x} = N^{w}_{c,u}/N^{w}_{tot,c}$ and $\mathbf{y} = N^{\overline{w}}_{c,u}/N^{\overline{w}}_{tot,c}$ denote the load created by user u at its original band and its target band. For a successful HO operation we expect that the intra-cell LB index gets smaller after intra-cell HO operation, that is $J^{after}_{intra} < J^{before}_{intra}$. Then the following equality given (4.14) should be satisfied. The left handside of the equality is the gain of switching a CBR user u from band w to $\overline{w}$

$$\frac{2(LOAD^{w}_{c} - LOAD^{\overline{w}}_{c})}{\mathbf{x}+\mathbf{y}} > 1. \tag{4.14}$$

Now the intra-cell LB procedure for cell c are summarized with the following steps:

(i) Calculate the virtual load of inner and outer band.
- If the load of inner band is greater than the outer band, decrease the temporary $R^{temp}_{int,c}$ in steps of Δ_{intra}.
- If the load of outer band is greater than inner band, increase the temporary $R^{temp}_{int,c}$ in steps of Δ_{intra}.

(ii) Determine candidate UE u which is expected to change its band if the current $R_{int,c}$ is updated to the temporarily adjusted $R^{temp}_{int,c}$.

(iii) For UE u check the intra-cell HO gain condition.
- If Equation 4.14 is satisfied, than the current $R_{int,c}$ is updated to the temporarily adjusted $R^{temp}_{int,c}$.
- Otherwise, current $R_{int,c}$ value is not updated.

5. SIMULATION RESULTS

5.1. Layout and Parameters

The simulation model has developed in MATLAB environment. The aim of the simulations is to observe the behavior of the implemented MLB algorithm when any of the cells is in overloaded state. In our network model depicted in Figure 5.1, the central cell, i.e. Cell 1, is an overloaded cell with 70 users and the adjacent neighboring cells of Cell 1, i.e. 2, 3, 4, 5, 6 and 7, are assumed to be relatively less loaded with the same number of users. According to number of users in each adjacent neighbor, four different cases are defined in order to see the change in the system behavior with respect to the user distribution in surrounding cells. These cases are Case 1, Case 2, Case 3 and Case 4 and in each cases there are 20, 25, 30 and 35 users placed on each adjacent neighboring cells, respectively and the rest of the cells are assumed to be very low loaded with 8 users. For all users, the employed service type is CBR with 256 kbps. In the case of SFR, power control factors of 1 and 4 are applied corresponding to edge user gains of 0 dB and 6 dB, respectively. Addtionally, initially the radius of the interior region is adjusted as 0.667 km for both SFR and FFR. General parameters used in simulations are detailed in Table 5.1.

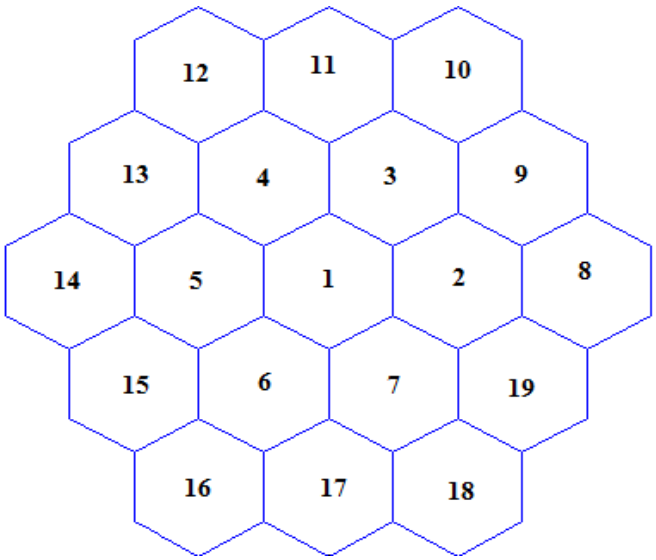

Figure 5.1. Network layout.

Table 5.1. Simulation parameters.

Parameter	**Value /Assumption**
Cell Layout	Hexagonal - Single Sector
User Distribution	Uniform
Inter-site Distance	1 Km
Cell Edge SINR	10 dB
System Bandwidth	10 MHz ($48 PRBs$)
N_{int}	24 PRBs
Traffic Model	256kbps CBR
CIO_{max}	6 dB
CIO_{min}	-6 dB
Δ	1 dB
Δ_{intra}	0.01 km
H	4 dB
$LOAD_{th}$	95% of total PRBs
$LOAD_{th,HO}$	85% of total PRBs
$SINR_{th,min}$	-7.04 dB

Three different system types are configured to evaluate MLB performance. First system is without LB, second system is MLB 1 in which the overloaded cells can transfer some of their load to the first tier neighbors and third system represent MLB 2 in which non-adjacent neighbors are included in the optimization area. In the cases of FFR and SFR, MLB 1 and MLB 2 refers the cooperation of intra and inter-cell LB. In addition to MLB 1 and MLB 2, we also wanted to observe the affect of adjusting the interior radius on the cell-edge spectral efficiency of the overloaded cell. Therefore, differently from MLB 1 and MLB 2, we simulated another two systems where R_{int} is not modified and only inter-cell MLB is applied for FFR and SFR. When we only consider the inter-cell MLB for FFR and SFR, if only the adjacent neighbors are involved to the inter-cell MLB, we called the system as MLB 3 and if non-adjacent neighbors are also involved to the optimization area of inter-cell MLB, we called the system as MLB 4.

5.2. Performance Evaluation of MLB

MLB performance is evaluated based on the following metrics: inter-cell LB index, intra-cell LB index, number of unsatisfied users, mean spectral efficiency of the overloaded cell and thespectral efficiency total system.

(i) *Inter-Cell LB index:* Inter-cell LB index measures the degree of LB between cells. Jain's fairness index defined in Equation 5.1 is used as inter-cell LB index.

$$J(\widehat{LOAD})_{inter} = \frac{(\sum_{c=1}^{n} \widehat{LOAD}_c)^2}{|\mathbf{C}| \sum_{c=1}^{n} (\widehat{LOAD}_c)^2} \tag{5.1}$$

The inter-cell LB index takes value in the interval $\left[\frac{1}{\mathbf{C}}, 1\right]$. A larger index means a more balanced load distribution between cells. In contrast, when the load is unbalanced seriously, load balance index value becomes very close to the reciprocal of the total number of cells.

(ii) *Intra-Cell LB index:* Intra cell load balance index measures the degree of LB between the interior and exterior regions of a cell and defined as

$$J(\widehat{LOAD})_{intra}(x) = \frac{\sum_{c=1}^{n} (\widehat{LOAD}_{c,w} - \widehat{LOAD}_{c,\overline{w}})^2}{|\mathbf{C}|} \tag{5.2}$$

where $\overline{w}$ is the set opposite band to band w where one band is assigned to the interior region and the opposite band is assigned to the exterior region or vice versa. In the case of SFR, the interior region is assigned by a set of bands. The intra-cell LB index takes value in the interval $[0, 1]$ and a smaller index means a more balanced load distribution between the interior and exterior regions.

(iii) *Number of Unsatisfied Users:* In overloaded cells, some users cannot be served with their required service quality and called as unsatisfied users. According to [20], the number of unsatisfied users is calculated theoretically as in the following

equation

$$Z = \sum_{c} \max \left(\sum_{u \in \mathbf{U_c}} |\mathbf{U_c}| * \left(1 - \frac{1}{\overline{LOAD_c}} \right) \right). \tag{5.3}$$

According to the proposed in Equation 5.3, number of unsatisfied users is calculated based on the virtual load of the cell and that is why the number of unsatisfied users is independent of the scheduling method. Reduction in the number of unsatisfied users is used to compare different system types.

(iv) *User Spectral Efficiency:* When a user is handedover from its serving cell to a target cell, the amount of resources that scheduled to the user by the target cell will be different than the amount of resource scheduled by previously serving cell. In inter-cell LB the cell-edge users are forced to make HO from overloaded cell to relatively low loaded cell. Therefore, observing the empirical cumulative distribution function (ECDF) of cell-edge user spectral efficiency gives a clear indication about how MLB enhances the minimum achievable spectral efficiency of the users that locate far from their serving cells.

Additionally, we measure the mean spectral efficiency of all users connected to central cell and also cell-edge users of cental cell individually. Finally, we observe the spectral efficiency of total system.

5.2.1. Case 1

In Case 1, 70 users located in the the central cell and 20 users are located randomly on each adjacent neighbors of the central cell. Figure 5.2 depicts the inter-cell LB index among central cell, Cell 1, and its six adjacent neighbors varying with LB times for Case 1. Without MLB, inter-cell LB index takes the values between 0.67 and 0.70. The achieved inter-cell LB index is almost the same after MLB 1 and MLB 2 for FFR, SFR 0 dB and SFR 6 dB and reaches 1. On the other hand, inter-cell LB index is the lowest after MLB 1 for reuse-3. It is observed that MLB provides more balanced load distribution among neighboring cells.

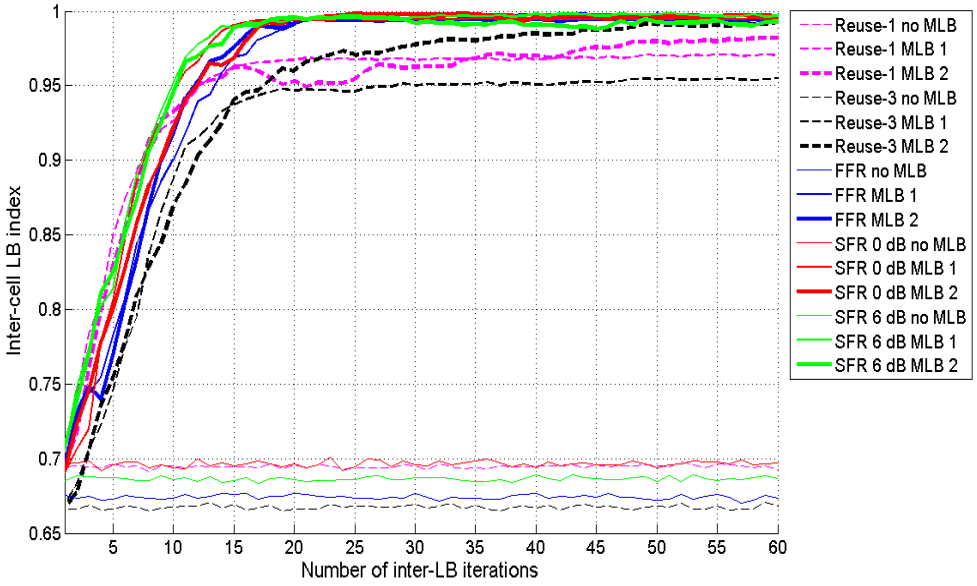

Figure 5.2. Inter-cell LB index varying load balancing iterations for Case 1.

Secondly, variation in the intra-cell LB index of the network is observed for FFR, SFR 0 dB and SFR 6 dB in Figure 5.3 for Case 1. In the case of SFR 0 dB, the power control factor is 1 that means there is no interference mitigation for the cell-edge users. Therefore, cell-edge users face with very low SINR and create higher load in outer band compared to inner band that is why intra-cell load index for SFR 0 dB is very high at the beginning. On the other hand, SFR 6 dB increases SINR values that cell-edge users measure with power factor 4. Consequently, the load is more balanced between inner and outer band for SFR 6 dB and intra-cell LB index is lower than FFR and SFR 0 dB. It is observed that MLB 1 and MLB 2 reduces the intra-cell LB index with the coordination of intra and inter LB. For example, for the overloaded cell intra-cell LB increases R_{int} and inter-cell MLB triggers HO operation for cell-edge users. Both of these actions decrease the load at the exterior region and help to provide balance between inner and outer bands of the central cell. While the cell-edge users of the cental cell are directed to its adjacent neighbors, the load of outer bands of the neighboring cells increase and causes load imbalance between inner and outer band of neighboring users. Since intra-cell LB activated in each neighboring cells individually amount of load difference created in neighboring cells is less than the amount of load difference decreased in the central cell. As a result, intra-cell LB index is decreasing very fast

while the overloaded central-cell is directing its cell-edge users to its neighboring cells and after all the cell-edge users are directed to the neighbors, we observe a bit increment in the intra-cell LB index which is caused by created load imbalance in the neighboring cells.

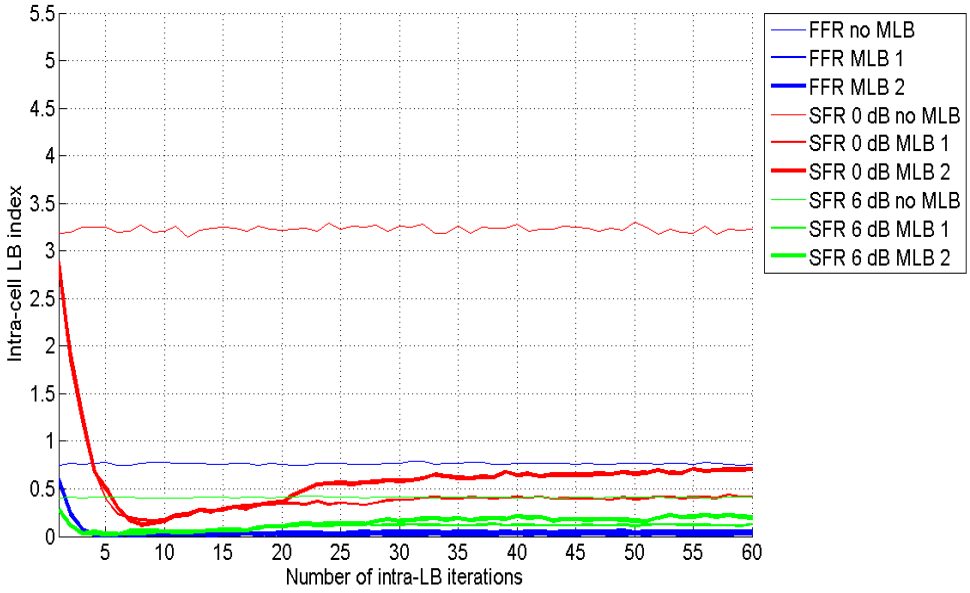

Figure 5.3. Intra-cell LB index varying load balancing iterations for Case 1.

Figure 5.4 shows the theoretically calculated number of unsatisfied users in Cell 1 for three system types for different frequency planning schemes. Results show that in Case 1, gain of MLB 1 over no MLB is 70% for reuse-1 and reuse-3, 90% for SFR 0 dB, 100% for FFR and SFR 6 dB. There is no unsatisfied users remain after MLB 2 for reuse-1, FFR, SFR 0 dB and SFR 6 dB. In other words, Cell 1 is not overloaded anymore after MLB 2. On the other hand, the gain of MLB 2 is 95% for reuse-3.

Figure 5.5, shows the ECDF of cell-edge users spectral efficiency of Cell 1 for round robin scheduler for Case 1. Without MLB, the cell-edge spectral efficiency takes the values between 0.30 - 0.55 bits/s/Hz on average in Case 1. MLB 1 enhances the cell-edge spectral efficiency for each frequency planning schemes. The minimum throughput that 50% of cell-edge users achieve becomes 0.63, 0.78, 1, 1.3 and 1.5 bits/s/Hz for reuse-1, reuse-3, SFR 0 dB, SFR 6 dB and FFR, respectively. In Case 1, each surrounding cell has 20 users and has available resources to serve new coming

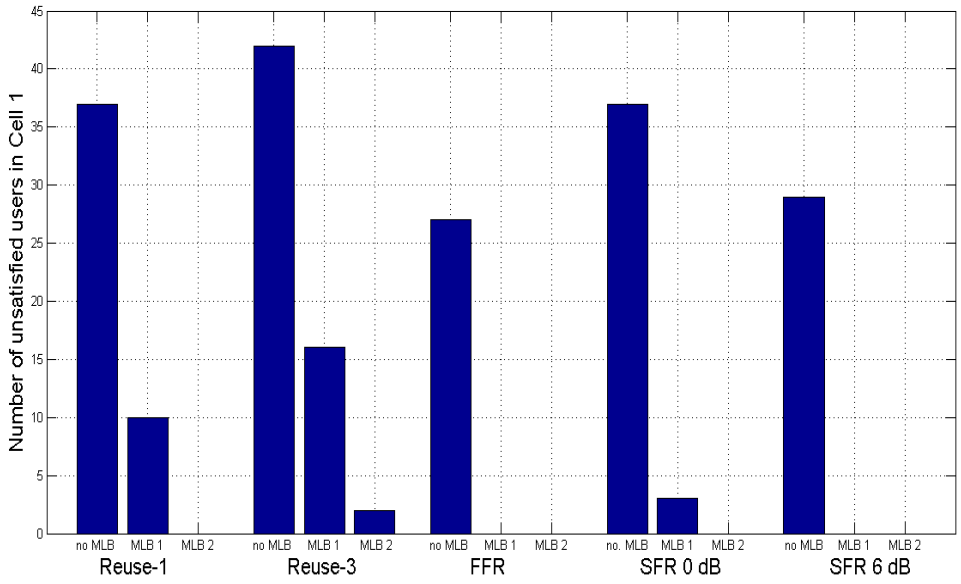

Figure 5.4. Number of unsatisfied users in Cell 1 for Case 1.

users. As a result, most of the cell-edge users which create overload condition in Cell 1 can be handedover to the adjacent neighbors with MLB 1. That is why the performances of MLB 1 and MLB 2 are very close for reuse-1 and reuse-3 and almost the same for FFR, SFR 0 dB and SFR 6 dB.

In Figure 5.6 MLB performances of different frequency planning schemes are compared for the proportional fair scheduler. Without MLB minimum cell-edge throughput that 50% of the cell-edge users achieve reside between 0.9 - 1.4 bits/s/Hz. MLB 1 brings the minimum achievable throughput between 2.1 and 2.6 bits/s/Hz for 50% of the cell-edge users where SFR 6 dB and FFR reach the highest throughput whereas reuse-3 gives the lowest. The achievable spectral efficiency values are the same after MLB 1 and MLB 2 for reuse-1, FFR, SFR 0 dB and SFR 6 dB. Only for reuse-1 MLB 2 performs better than MLB 1.

The results of Case 1 for the best-CQI scheduler for different frequency planning schemes are illustrated in Figure 5.7. Since Best-CQI scheduler allocates resources to the user with best channel conditions, cell-edge users are not scheduled for reuse-1 and reuse-3. However, for FFR and SFR, inner and outer bands schedule the users

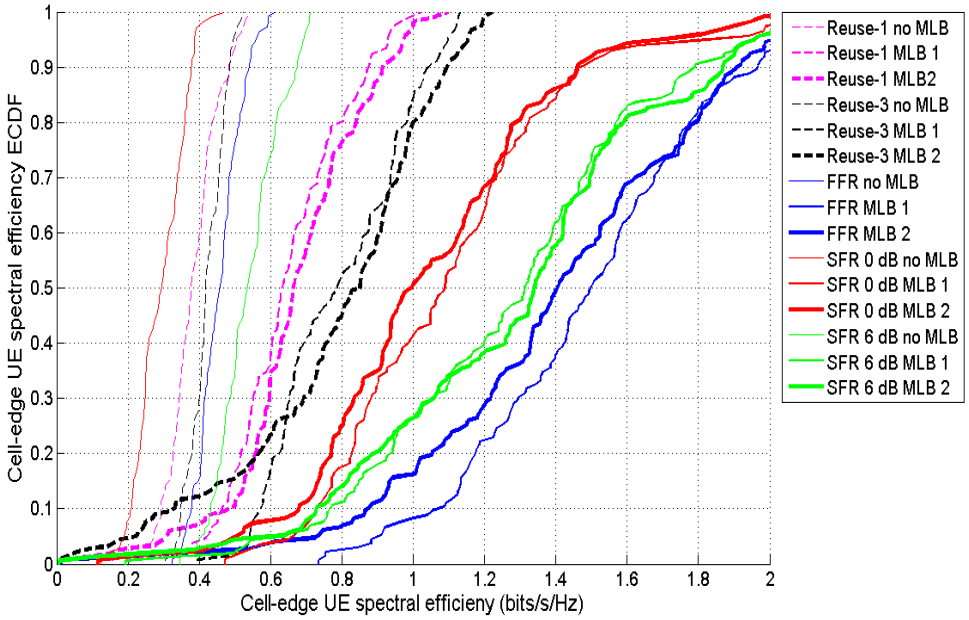

Figure 5.5. Performance of MLB with round-robin scheduler for different frequency planning schemes for Case 1.

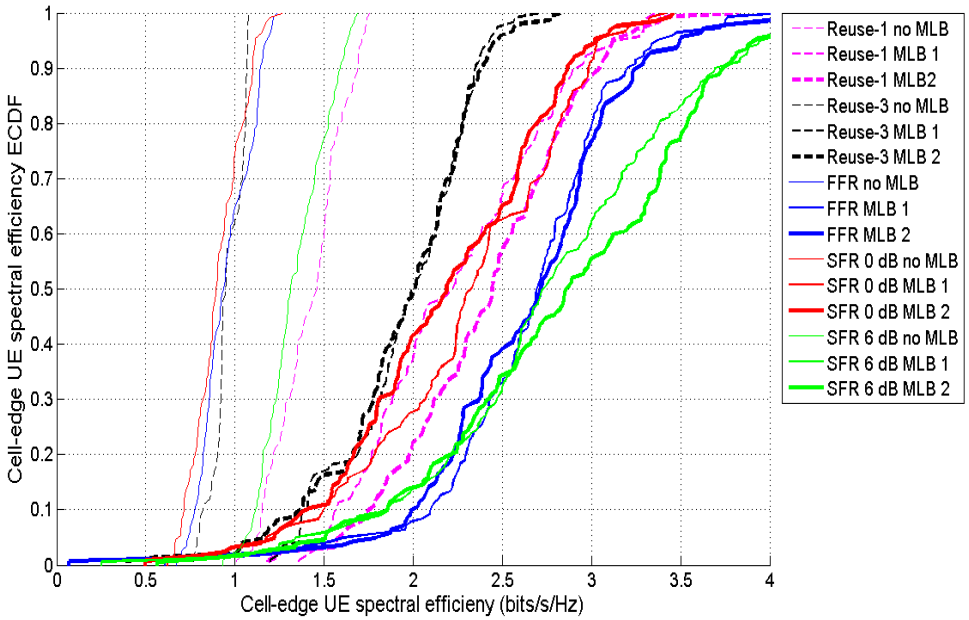

Figure 5.6. Performance of MLB with proportional fair scheduler for different frequency planning schemes for Case 1.

individually so that it can be observed that some cell-edge users locate in the outer band and have relatively better channel conditions are likely to be scheduled. We see

that spectral efficiency is improved with best-CQI scheduling with the help of MLB 1 and MLB 2. It is also observed that MLB 1 for SFR 0 dB performs better than FFR and SFR 6 dB for minimum achievable spectral efficiency of 50% of the users. When it comes the peak spectral efficiency of cell-edge users SFR 6 dB is better than FFR and SFR 0 dB. Best-CQI achieves higher peak spectral efficiency than other schedulers.

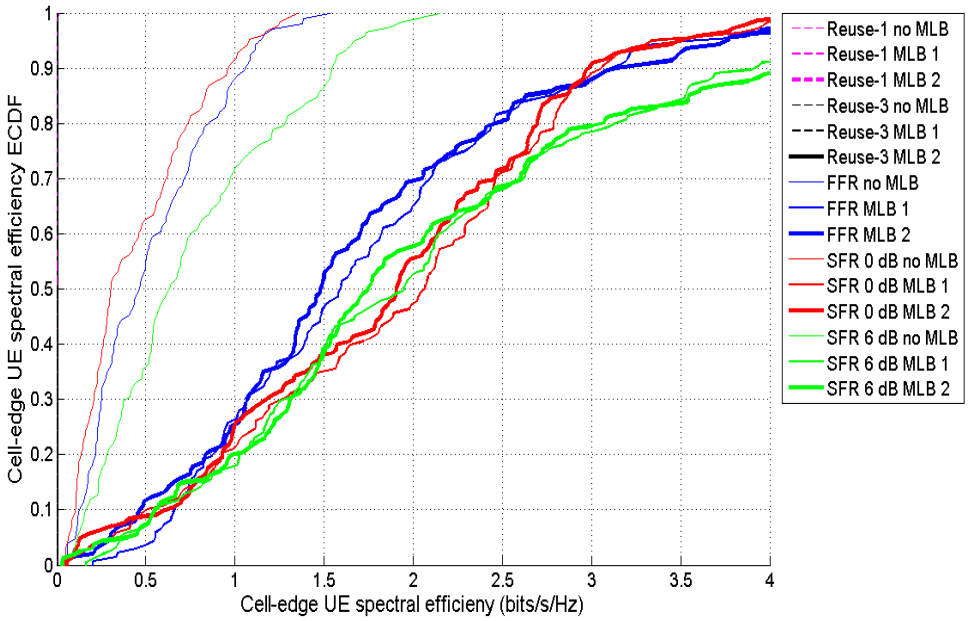

Figure 5.7. Performance of MLB with best-CQI scheduler for different frequency planning schemes for Case 1.

In Table 5.2, the mean bandwidth efficiency values of cell-edge users of Cell 1 for three system types are listed for different frequency schemes and for round-robin and proportional fair scheduler, respectively. When we compare two scheduler, we observe that proportional fair scheduler achieve higher mean cell-edge spectral efficiency for all frequency planning schemes than the round-robin scheduler. For round-robin scheduler reuse-1 performs worst and FFR performs best among all frequency planning schemes. In the case of the proportional fair scheduler, SFR 6 dB outperforms the other schemes while FFR is the second in terms of the mean cell-edge spectral efficiency. In Case 1, adjacent neighbors have some available capacity for cell-edge users of central cell so the MLB 1 is very efficient even performances of MLB 1 and MLB 2 are almost the same. As stated before, for cell-edge user bandwidth efficiency, we define MLB 3 and

Table 5.2. Mean spectral efficiency of cell-edge users of Cell 1 in bits/s/Hz for Case 1 for different schedulers and frequency planning schemes.

		Reuse-1	Reuse-3	FFR	SFR 0 dB	SFR 6 dB
Round-robin scheduler	no MLB	0.39	0.42	0.46	0.29	0.53
	MLB 1	0.65	0.80	1.45	1.11	1.29
	MLB 2	0.68	0.78	1.41	1.05	1.30
	MLB 3	0.65	0.80	0.70	0.48	0.69
	MLB 4	0.68	0.78	1.07	0.51	0.69
Proportional fair scheduler	no MLB	1.42	0.96	0.97	0.90	1.38
	MLB 1	2.25	1.97	2.65	2.30	2.79
	MLB 2	2.42	1.95	2.65	2.18	2.76
	MLB 3	2.25	1.97	1.48	1.40	1.84
	MLB 4	2.42	1.95	1.51	1.47	1.89

MLB 4 to understand the effect of intra-cell LB. In the cases of FFR and SFR, when we take a look at the results for MLB 3 and MLB 4, it is seen that MLB 1 achieves higher bandwidth efficiency than MLB 3 achieves higher spectral efficiency than MLB 4. These results prove that is the R_{int} is not adjusted for LB purposes the gain of MLB reduces. Since for all four systems MLB refers inter-cell MLB for reuse-1 and reuse-3, the results are the same for MLB 1 and MLB 3 and for MLB 2 and MLB 4 for reuse-1 and reuse-3.

In Table 5.3, we can see the effect of MLB 1 and MLB 2 on the total system spectral efficiency in kbits/s/Hz for Case 1 for different frequency planning schemes and schedulers. For the scheduling methods which consider fairness among users, because of the new coming user the resource remaining for existing users of an adjacent neighbor reduces. This results with a bit degradation in total system spectral efficiency of the network. Additionally, it is noticed that for best-CQI scheduling, bandwidth efficiency is not affected by MLB 1 and MLB 2 for reuse-1 and reuse-3 so the total system spectral efficiency is also unchanged. On the other hand, best-CQI scheduler gives the higher total system spectral efficiency than round-robin and proportional fair schedulers.

Table 5.3. Total system spectral efficiency in kbits/s/Hz for Case 1 for different schedulers and frequency planning schemes.

		Reuse-1	Reuse-3	FFR	SFR 0 dB	SFR 6 dB
Round-Robin Scheduler	no MLB	1.85	1.04	1.72	2.03	1.81
	MLB 1	1.83	1.03	1.43	1.54	1.36
	MLB 1	1.75	0.99	1.40	1.52	1.36
Proportional fair Scheduler	no MLB	3.17	1.51	2.50	3.15	2.96
	MLB 1	3.12	1.48	2.18	2.53	2.38
	MLB 2	2.88	1.40	2.19	2.51	2.32
Best-CQI Scheduler	no MLB	4.57	1.67	2.82	3.54	3.48
	MLB 1	4.57	1.67	2.71	3.27	3.28
	MLB 2	4.57	1.67	2.70	3.25	3.25

5.2.2. Case 2

In Case 2, 70 users located in the the central cell and 25 users are located randomly on each adjacent neighbors of the central cell. Figure 5.8 depicts the inter-cell LB index among central cell, Cell 1, and its six adjacent neighbors varying with LB times for Case 2. Without MLB, inter-cell LB index takes the values around 0.78 which is greater than Case 1. When MLB 1 is applied, FFR achieves the highest inter-cell LB index with the value of 0.99. Inter-cell LB index, for SFR 0 dB and SFR 6 dB are close to FFR whereas reuse-1 and reuse-3 only achieve 0.86 and 0.91 after MLB 1, respectively. After MLB 2, FFR, SFR0 dB and SFR 6 dB provides same degree of LB with inter-LB index close to 1 and reuse-1 and reuse-3 achieves 0.98. Results show that load is more balanced among adjacent neighbors for FFR and when only MLB 1 is applied. On the other hand, FFR, SFR 0 dB and SFR 6 dB provide same degree of load balance after MLB 2. In both MLB 1 and MLB 2, reuse-1 and reuse-3 provide less balanced load distribution than other frequency planning schemes.

Figure 5.9 illustrates the intra-cell LB index of the network varying with load balancing times for Case 2. As explained in Case 1, for SFR 6 dB the load difference

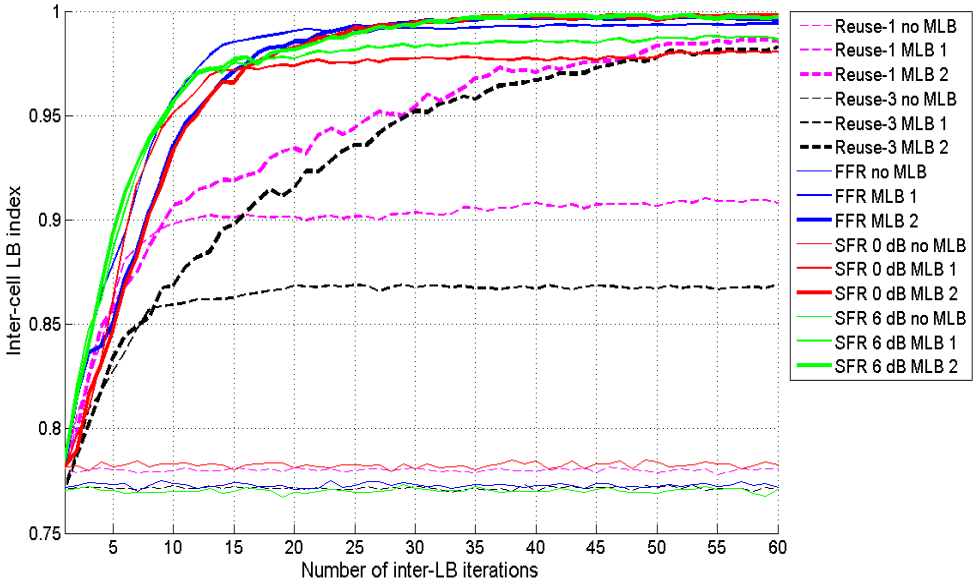

Figure 5.8. Inter-cell LB index varying load balancing iterations for Case 2.

between the interior and exterior regions is more than FFR and SFR 0 dB and therefore intra-cell LB index takes the highest value for SFR 6 dB. Additionally, we again observe that intra-cell LB index is decreasing very fast while the overloaded central-cell is directing its cell-edge users to its neighboring cells and after all the cell-edge users are directed to the neighbors in the expense of a bit increment in the intra-cell LB index which is caused by created load imbalance in the neighboring cells.

Figure 5.10 shows the theoretically calculated number of unsatisfied users in Cell 1 for three system type for different frequency planning schemes for Case 2. Results show that in Case 2 gain of MLB 1 is less than the gain achieved in Case 1 for all frequency planning schemes. More specifically, for MLB 1 the gain is the highest for FFR and the lowest for reuse-3 with 88% and 20%, respectively. On the other hand, there is no unsatisfied users remain after MLB 2 for FFR, SFR 0 dB and SFR 6 dB.

Figure 5.11, shows the ECDF of cell-edge user spectral efficiency of Cell 1 for round robin scheduler. Without MLB, minimum achieved cell-edge throughput takes the values between 0.25 - 0.5 bits/s/Hz for 50% of the cell-edge users in Case 2. MLB 1 enhances the cell-edge throughput for each frequency planning schemes and the min-

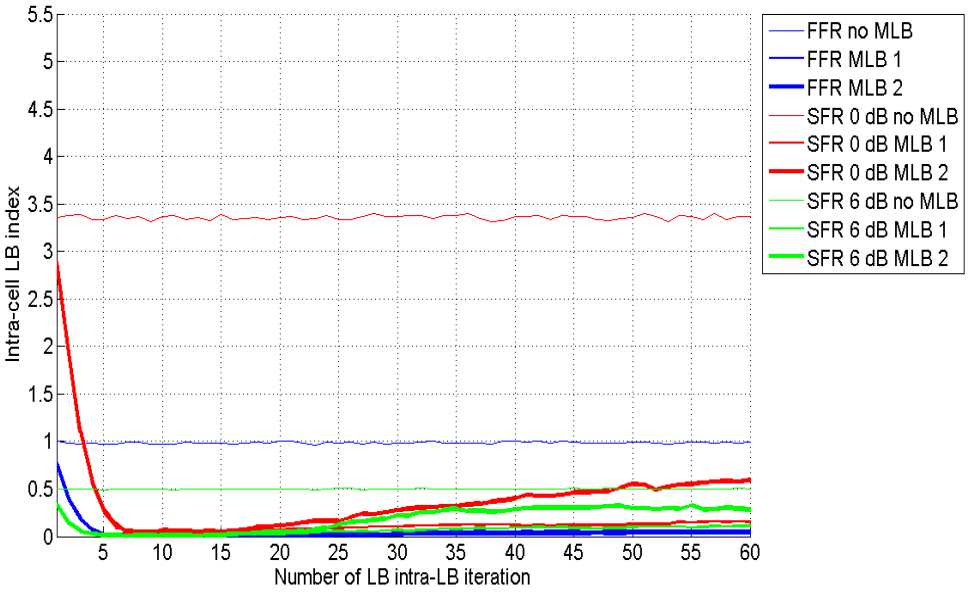

Figure 5.9. Intra-cell LB index varying load balancing iterations for Case 2.

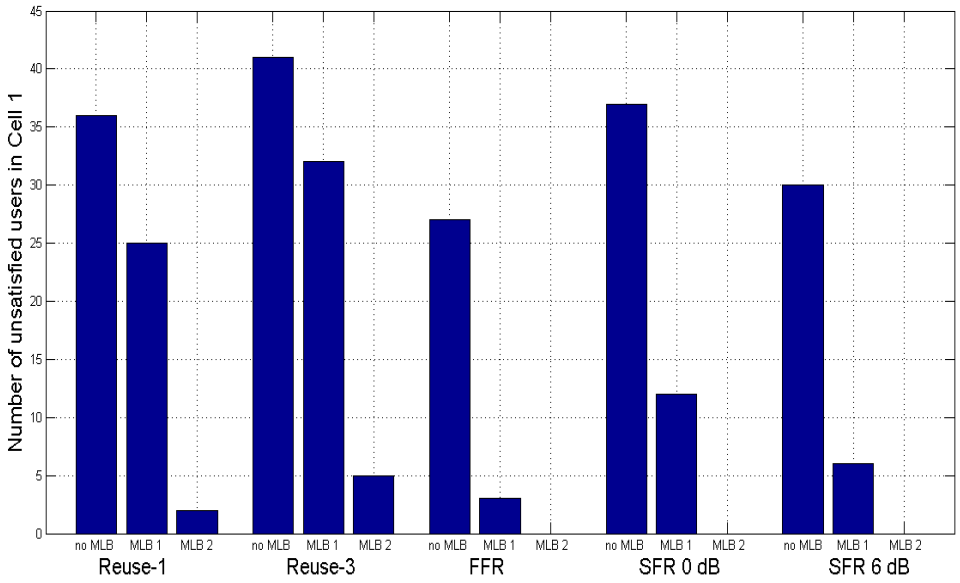

Figure 5.10. Number of unsatisfied users in Cell 1 for Case 2.

imum throughput that 50% of the cell-edge users achieve becomes 0.5 bits/s/Hz for reuse-1 and reuse-3, 1.1 bits/s/Hz for SFR 6 dB and SFR 0 dB and 1.3 for FFR. In Case 2, the adjacent neighbors of central cell are high loaded with 25 users for reuse-1 and reuse-3. Consequently, Cell 1 requires sec. MLB for extra capacity to direct all the cell-edge users to adjacent neighbors. That is why the performance of MLB 2 is

better than MLB 1 for reuse-1 and reuse-3. On the other hand, the spectral efficiency gains of MLB 1 and MLB 2 are very close to each other for FFR, SFR 0 dB and SFR 6 dB. In addition, it is observed that for both MLB 1 and MLB 2, FFR outperforms the other frequency planning schemes in Case 2.

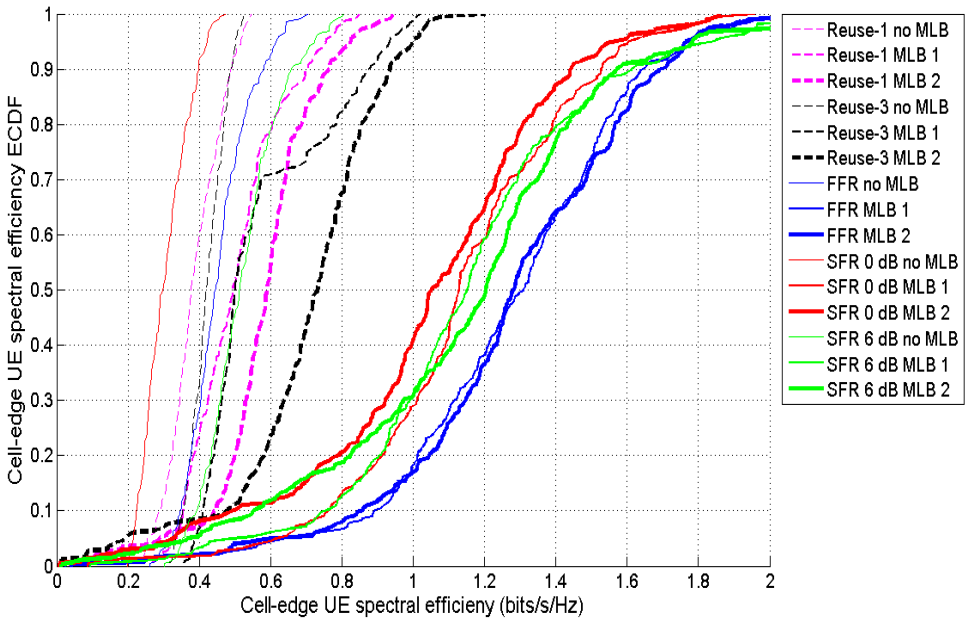

Figure 5.11. Performance of MLB with round-robin scheduler for different frequency planning schemes for Case 2.

Figure 5.12 compares the MLB performance of proportional fair for different frequency planning schemes for Case 2. Without MLB cell-edge spectral efficiencies reside between 0.9 - 1.4 bits/s/Hz. As in round-robin scheduler, the performance gain of MLB 2 is higher than MLB 1 for both reuse-1 and reuse-3. In contrast, the minimum cell-edge spectral efficiency that 50% of the users achieve is almost the same after MLB 1 for SFR 0 dB, SFR 6 dB and FFR with 2.5 bits/s/Hz. On the other hand, SFR 6 dB outperforms the other frequency planning schemes with 2.6 bits/s/Hz on the average.

The results of Case 2 for the best-CQI scheduler for different frequency planning schemes are illustrated in Figure 5.13. It is observed that MLB 1 for SFR 0 dB performs better than FFR and SFR 6 dB for 50% of the users. When it comes the peak spectral efficiency SFR 6 dB is the best among FFR and SFR 0 dB.

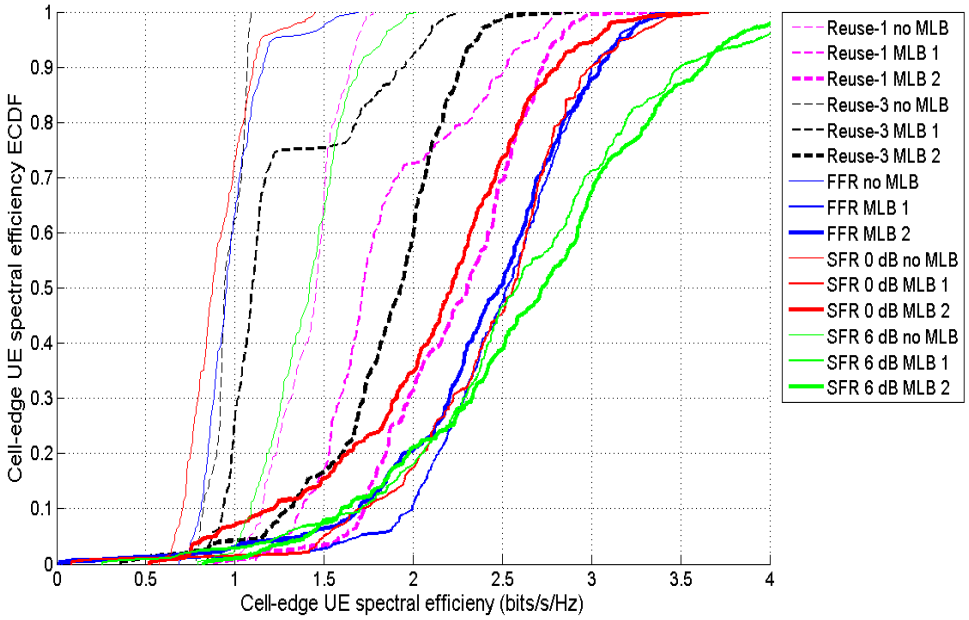

Figure 5.12. Performance of MLB with proportional fair scheduler for different frequency planning schemes for Case 2.

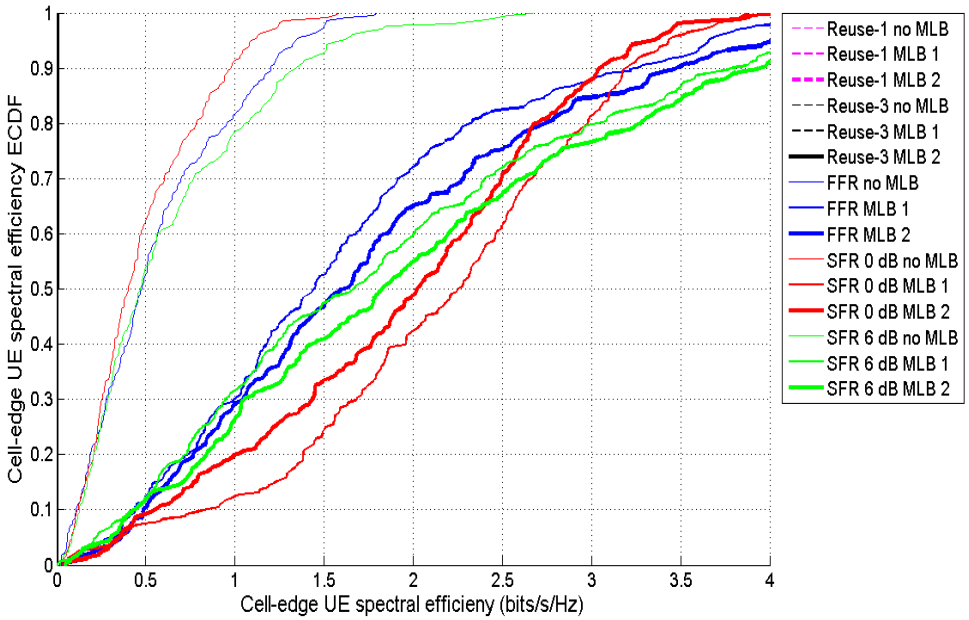

Figure 5.13. Performance of MLB with best-CQI scheduler for different frequency planning schemes for Case 2.

In Table 5.4, the mean bandwidth efficiency values of cell-edge users of Cell 1 for three system type are listed for different frequency schemes and for round-robin

and proportional fair scheduler, respectively for Case 2. As in Case 1, we observe that proportional fair scheduler achieve higher mean cell-edge spectral efficiency for all frequency planning schemes than the round-robin scheduler. Under round-robin scheduler reuse-1 performs worst and FFR performs best among all frequency planning schemes. In the case of proportional fair scheduler SFR 6 dB outperforms the other schemes while FFR is the second in terms of mean cell-edge spectral efficiency. Differently from Case 1, it is seen that MLB 2 performs better than MLB 1 for reuse-1 and reuse-3 whereas for other frequency planning schemes performance of MLB methods are the same or MLB 1 is better. The reason is that MLB 2 is activated as soon as total virtual load of adjacent neighbors exceed $LOAD_{HO}$ to create available capacity in these neighbors. On the other hand, intra-LB alone can also change the virtual load of a cell with intra-cell HOs and achieves the same mean cell-edge spectral efficiency as MLB 2 in Case 1 and Case 2. In the cases of FFR and SFR, when we take a look at the results for MLB 3 and MLB 4, it is seen that MLB 1 achieves higher bandwidth efficiency than MLB 3 achieves higher spectral efficiency than MLB 4. It shows that using intra-LB in coordination with inter-MLB is highly effective.Since for all four systems MLB refers inter-cell MLB for reuse-1 and reuse-3, the results are the same for MLB 1 and MLB 3 and for MLB 2 and MLB 4 for reuse-1 and reuse-3.

In Table 5.5, we can see the effect of MLB 1 and MLB 2 on the total system throughput in kbits/s/Hz for Case 2 for different frequency planning schemes and schedulers.

5.2.3. Case 3

In Case 3, 70 users located in the the central cell and 30 users are located randomly on each adjacent neighbors of the central cell. Figure 5.14 depicts the inter-cell LB index among central cell, Cell 1, and its six adjacent neighbors varying with LB times. It is observed that inter-cell LB index of MLB 2 is the highest and no MLB is the lowest for each frequency planning scheme. Without MLB, inter-cell LB index takes the values between 0.81 and 0.86. More specifically, after MLB 1, FFR and SFR 6 dB outperforms all the other schemes and reaches the value of provide same degree

Table 5.4. Mean spectral efficiency of cell-edge users of Cell 1 in bits/s/Hz for Case 2 for different schedulers and frequency planning schemes.

		Reuse-1	Reuse-3	FFR	SFR 0 dB	SFR 6 dB
Round-robin scheduler	no MLB	0.39	0.42	0.46	0.29	0.53
	MLB 1	0.51	0.58	1.27	1.14	1.16
	MLB 2	0.58	0.70	1.29	1.05	1.14
	MLB 3	0.51	0.58	0.69	0.49	0.69
	MLB 4	0.58	0.70	0.71	0.53	0.69
Proportional fair scheduler	no MLB	1.42	0.96	0.97	0.90	1.38
	MLB 1	1.84	1.25	2.49	2.45	2.61
	MLB 2	2.24	1.85	2.40	2.13	2.67
	MLB 3	1.84	1.25	1.43	1.38	1.79
	MLB 4	2.24	1.85	1.46	1.41	1.82

Table 5.5. Total system spectral efficiency kbits/s/Hz for Case 2 for different schedulers and frequency planning schemes.

		Reuse-1	Reuse-3	FFR	SFR 0 dB	SFR 6 dB
Round-Robin Scheduler	no MLB	1.83	1.04	1.65	2.10	1.78
	MLB 1	1.82	1.03	1.35	1.60	1.38
	MLB 2	1.70	0.97	1.34	1.57	1.34
Proportional fair Scheduler	no MLB	3.31	1.50	2.52	3.17	2.9.0
	MLB 1	3.28	1.49	2.21	2.54	2.40
	MLB 2	2.97	1.35	2.18	2.49	2.35
Best-CQI Scheduler	no MLB	4.61	1.66	2.88	3.66	3.55
	MLB 1	4.61	1.66	2.77	3.40	3.32
	MLB 2	4.61	1.66	2.75	3.36	3.29

of load balance after MLB 2. In the cases of reuse-1 and reuse-3, since some of the neighboring cell are overloaded with 30 users activation of MLB 1 directs some of the load of adjacent neighbors to their adjacent neighbors and the load difference between central cell and its adjacent neighbors and so as the inter-cell index decrease at the

beginning and than not improve. On the other hand, when MLB 2 is applied inter-cell LB index is increased.

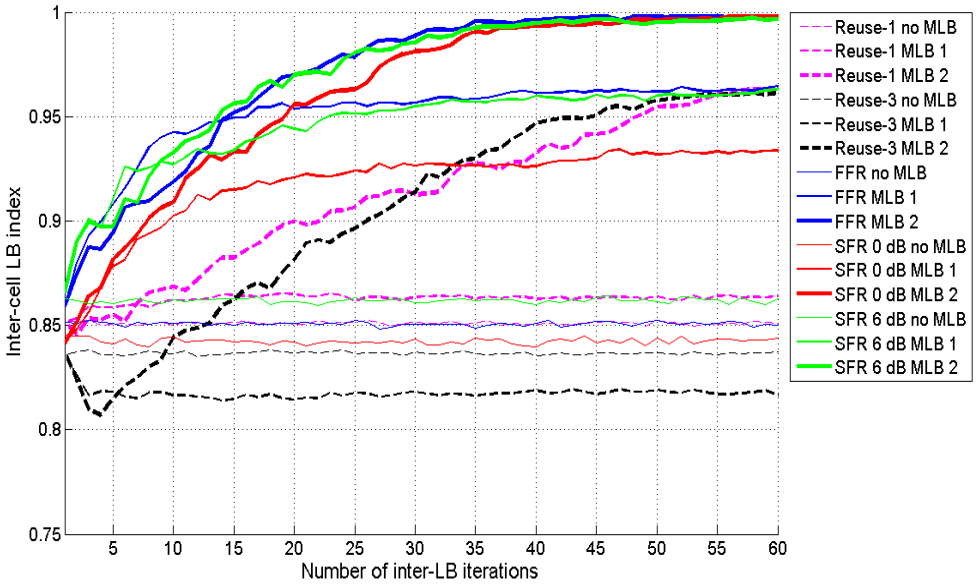

Figure 5.14. Inter-cell LB index varying load balancing iterations for Case 3.

Figure 5.15 illustrates the intra-cell LB index of the network varying with load balancing times for Case 3. As explained in previous cases, SFR 6 dB takes the highest value for intra-cell LB. Additionally, we observe that as the number of users reside in adjacent neighboring cells increases the intra-cell LB index values for SFR and FFR are higher than the previous cases at the beginning of LB operation and also the increment that we observe in the intra-cell LB index after the cell-edge users of overloaded cell is directed to neighbor cell is less compared to previous cases due to the fact that since the adjacent neighbors are accept less number of users since they are already high loaded, the load difference created in neighboring cells is also less.

Figure 5.16 shows the theoretically calculated number of unsatisfied users in Cell 1 for three system type for different frequency planning schemes for Case 3. Results show that in Case 3 gain of MLB 1 is too little for most of the frequency planning schemes. The gains of MLB 2 over no MLB are 73% and 67% for reuse-1 and reuse-3. On the other hand, there is no unsatisfied users remain after MLB 2 for FFR, SFR 0 dB and SFR 6 dB. In other words, Cell 1 is not overloaded anymore after MLB 2.

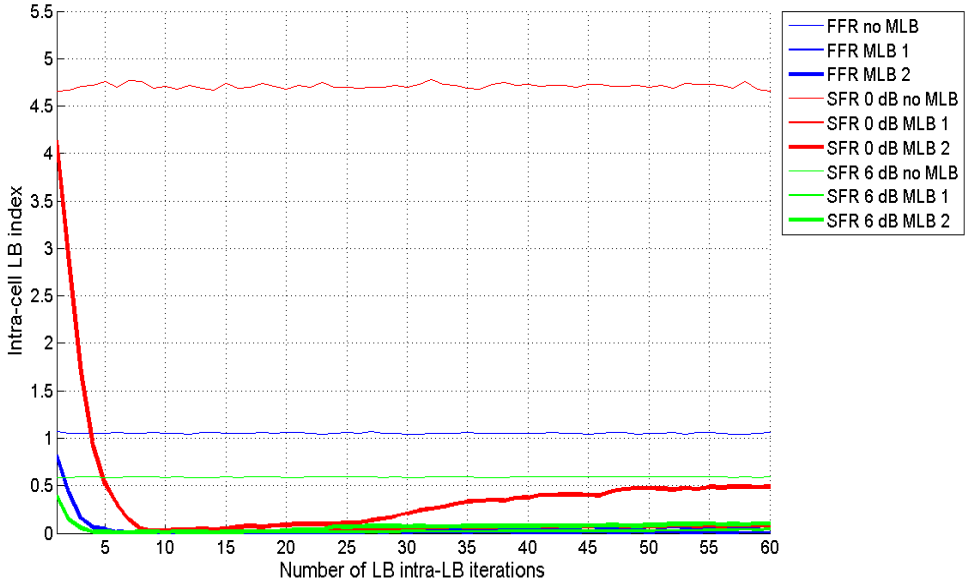

Figure 5.15. Intra-cell LB index varying load balancing iterations for Case 3.

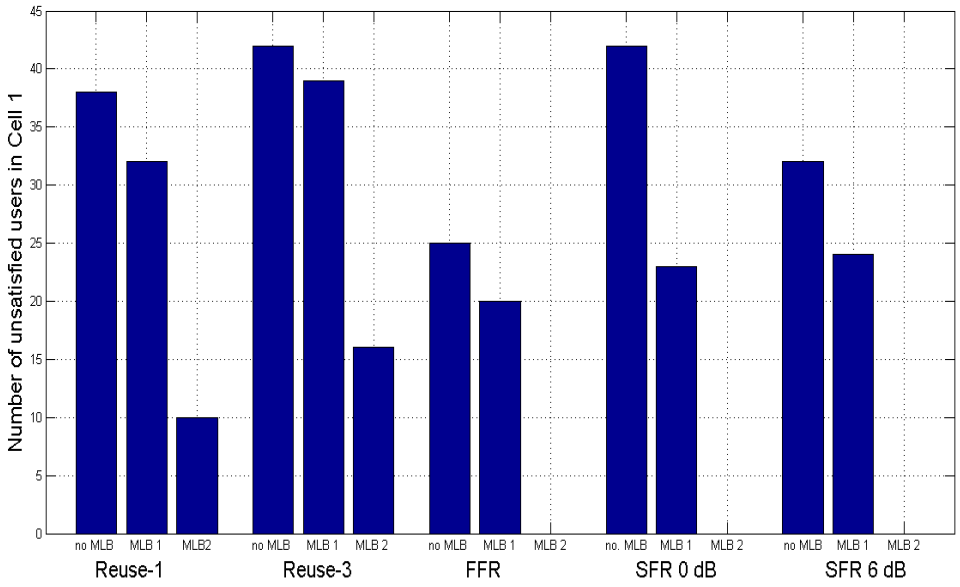

Figure 5.16. Number of unsatisfied users in Cell 1 for Case 3.

Figure 5.17 shows the ECDF function of cell-edge user spectral efficiency of Cell 1 for round robin scheduler. Without MLB, the cell-edge spectral efficiency takes the values between 0.25 - 0.5 bits/s/Hz in Case 3. MLB 1 can not improve the cell-edge spectral efficiency for reuse-1 and reuse-3 since the surrounding cells are in high or over-loaded state with 30 users. On the other hand, MLB 1 brings the minimum cell-edge

spectral efficiency to between 0.86 - 0.97 bits/s/Hz for other frequency planning schemes for 50% of the cell-edge users. Additionally, MLB 2 brings the minimum cell-edge spectral efficiency to 0.50 and 0.65 bits/s/Hz under reuse- 1 and reuse-3 and between 0.98 - 1.22 bits/s/Hz for SFR 0 dB, FFR and SFR 6 dB schemes. We can conclude that FFR performs better than other frequency planning approaches for round-robin scheduler by noting that without MLB 50% of the cell-edge users can not achieve more than 0.45 bits/s/Hz for FFR, after MLB 1 and MLB 2 the minimum achievable spectral efficiency becomes 1 bits/s/Hz and 1.22 bits/s/Hz, respectively. In contrast, reuse-1 gives the lowest spectral efficiency after application of MLB techniques.

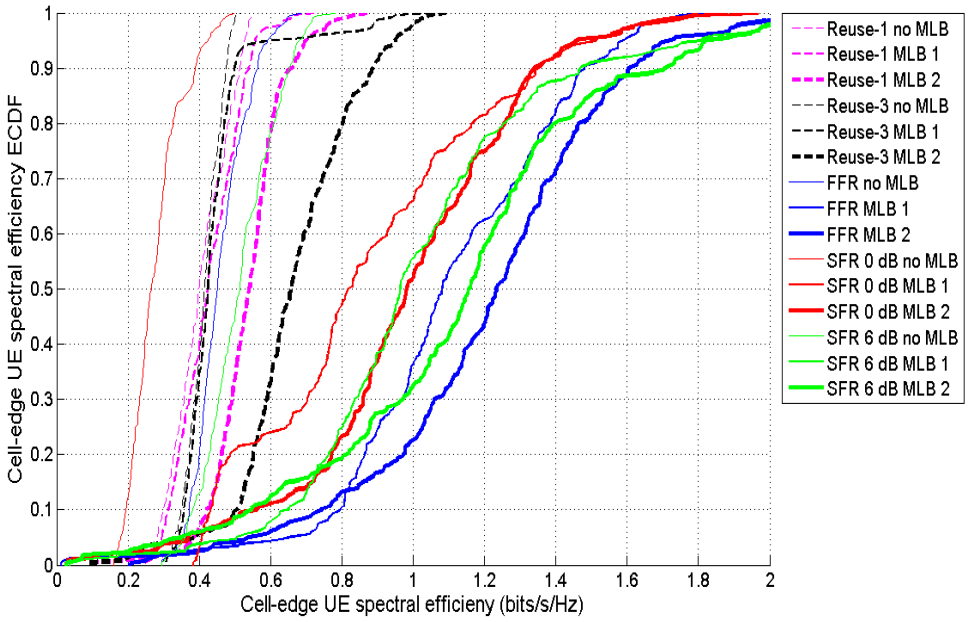

Figure 5.17. Performance of MLB with round-robin scheduler for different frequency planning schemes for Case 3.

Figure 5.18 compares the MLB performance of proportional fair for different frequency planning schemes for Case 3. Without MLB cell-edge spectral efficiencies reside between 0.9 - 1.4 bits/s/Hz. MLB 1 can not improves the cell-edge spectral efficiency for reuse-1 and reuse-3 as in round-robin scheduling. However, for the other frequency planning schemes, MLB 1 brings the cell-edge spectral efficiency to between 1.8 bits/s/Hz and 2.2 bits/s/Hz. In the case of MLB 2, 50% of the cell-edge users achieve more than 1.6 bits/s/Hz for reuse-1 and reuse-3 and minimum 2.2 bits/s/Hz

for other frequency planning schemes. SFR 6 dB outperforms all the other frequency planning schemes in both MLB 1 and MLB 2. In more detail, without MLB 50% of the cell-edge users can not achieve more than 1.45 bits/s/Hz for SFR 6 dB, after MLB 1 and MLB 2 the minimum achievable spectral efficiency becomes 2 bits/s/Hz and 2.5 bits/s/Hz, respectively. In contrast, reuse-3 gives the lowest throughput after application of MLB techniques.

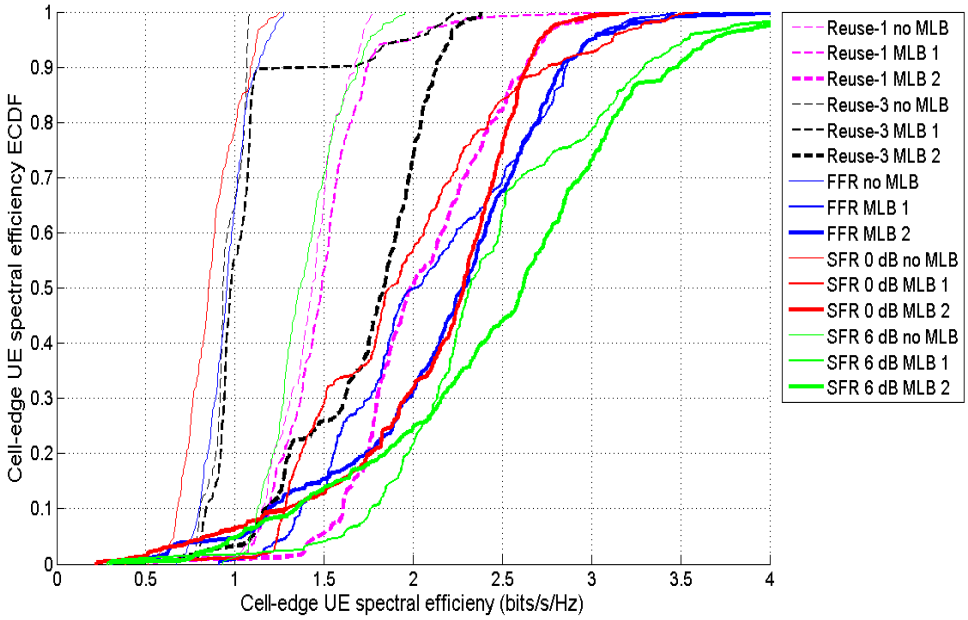

Figure 5.18. Performance of MLB with proportional fair scheduler for different frequency planning schemes for Case 3.

The results of Case 3 for the best-CQI scheduler for different frequency planning schemes are illustrated in Figure 5.19. We also observe that spectral efficiency is improved for cell-edge users for best-CQI scheduling with the help of MLB 1 and MLB 2.

In Table 5.6, the mean bandwidth efficiency values of cell-edge users of Cell 1 for three system type are listed for different frequency schemes and for round-robin and proportional fair scheduler, respectively for Case 3. In Case 3, the adjacent neighbors are high loaded and that is why MLB 2 performs better than MLB 1 for all frequency planning schemes and the two scheduling strategies. As in the previous cases, MLB 3

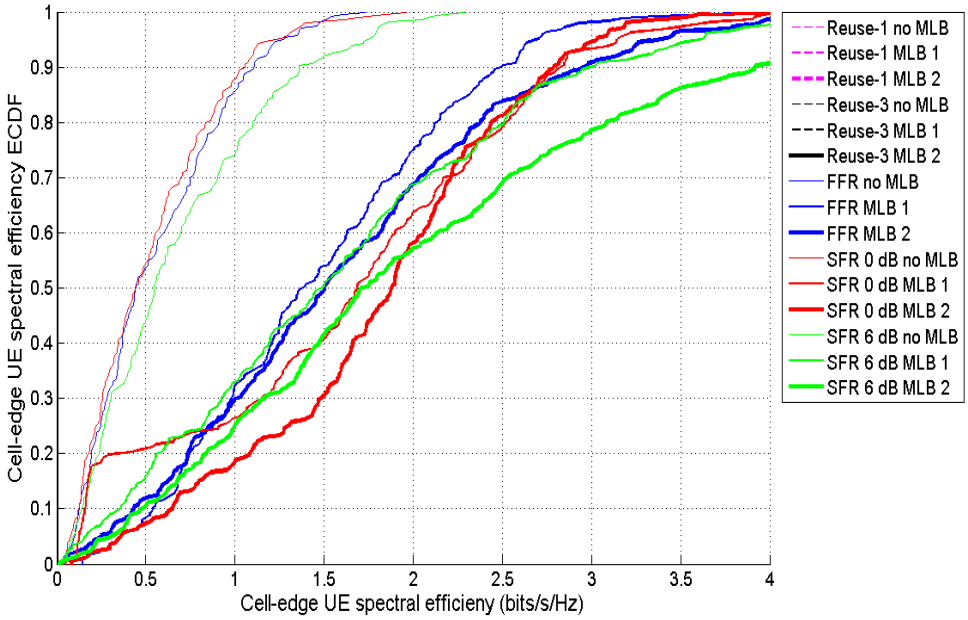

Figure 5.19. Performance of MLB with best-CQI scheduler for different frequency planning schemes for Case 3.

achieves less that MLB 1 and MLB 4 achieves less than MLB 2 in terms of cell-edge spectral efficiency for reuse-1 SFR and FFE whereas the results are the same for MLB 1 and MLB 3 and for MLB 2 and MLB 4 for reuse-1 and reuse-3.

In Table 5.7, we can see the effect of MLB 1 and MLB 2 on the total system spectral efficiency in kbits/s/Hz for Case 3 for different frequency planning schemes and schedulers.

5.2.4. Case 4

In Case 4, 70 users located in the the central cell and 35 users are located randomly on each adjacent neighbors of the central cell. Figure 5.20 depicts the inter-cell LB index among central cell, Cell 1, and its six adjacent neighbors varying with load balancing times. In Case 4, the adjacent neighbors of central cell are also in overloaded state with 35 users per cell. Due to the fact that adjacent cells are also overloaded, there is a smaller gap between load state of Cell 1 and its neighbors. As a result,

Table 5.6. Mean spectral efficiency of cell-edge users of Cell 1 in bits/s/Hz for Case 3 for different schedulers and frequency planning schemes.

		Reuse-1	Reuse-3	FFR	SFR 0 dB	SFR 6 dB
Round-robin scheduler	no MLB	0.39	0.42	0.46	0.29	0.53
	MLB 1	0.43	0.44	1.11	0.88	1.03
	MLB 2	0.54	0.67	1.2	0.99	1.13
	MLB 3	0.43	0.44	0.75	0.42	0.67
	MLB 4	0.54	0.67	0.76	0.45	0.68
Proportional fair scheduler	no MLB	1.42	0.96	0.97	0.90	1.38
	MLB 1	1.50	1.08	2.11	1.95	2.45
	MLB 2	2.06	1.74	2.18	2.11	2.5
	MLB 3	1.50	1.08	1.40	1.02	1.88
	MLB 4	2.06	1.74	1.50	1.21	1.90

Table 5.7. Total system spectral efficiency in kbits/s/Hz for Case 3 for different schedulers and frequency planning schemes.

		Reuse-1	Reuse-3	FFR	SFR 0 dB	SFR 6 dB
Round-Robin Scheduler	no MLB	1.85	1.01	1.68	2.02	1.82
	MLB 1	1.79	0.98	1.40	1.51	1.37
	MLB 2	1.66	0.93	1.33	1.45	1.28
Proportional fair Scheduler	no MLB	3.25	1.51	2.53	3.20	2.98
	MLB 1	3.21	1.48	2.26	2.60	2.55
	MLB 2	2.90	1.36	2.20	2.53	2.39
Best-CQI Scheduler	no MLB	4.60	1.67	2.90	3.62	3.63
	MLB 1	4.60	1.67	2.80	3.34	3.42
	MLB 2	4.60	1.67	2.75	3.30	3.33

without MLB, inter-cell LB index takes the values at around 0.83 which is higher than what MLB 1 and MLB 2 reach for reuse-1 and reuse-3. In the cases of reuse-1 and reuse-3, when MLB 1 is applied, the overloaded adjacent cells also transfer some of their excessive load to their neighboring cells and load states of adjacent neighbors of

Cell 1 decrease. Thus, the gap between load states of central cell and its neighbors becomes greater and inter-cell LB index reduces after MLB 1 for reuse-1 and reuse-3 although MLB 1 tries to solve the overload situation. When MLB 2 is applied, since more load is directed to the non-adjacent neighbors the load is more balanced among whole network. On the other hand, In the cases of SFR and FFR, the inter-cell LB index increase with LB iterations and SFR 6 dB reaches the highest inter-cell LB index after MLB 1. In the case of MLB 2 FFR, SFR 0 dB and SFR 6 dB provide same degree of load balance.

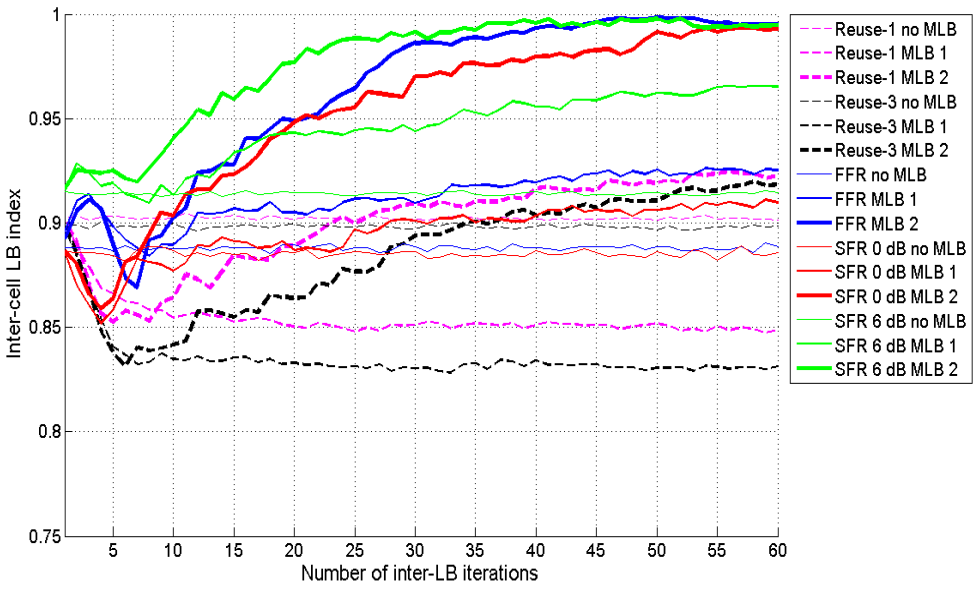

Figure 5.20. Inter-cell LB index varying load balancing iterations for Case 4.

Figure 5.21 illustrates the intra-cell LB index of the network varying with load balancing times for Case 4. In Case 4, SFR 6 dB takes the highest value for intra-cell LB among the other frequency planning schemes and previous cases which has less number of users in each adjacent neighbor of central cell. Additionally, the load difference created in neighboring cells is less than previous cases and therefore the final value for intra-cell LB index is the least for Case 4. Even FFR and SFR 6 dB have intra-cell LB index close to zero which means intra-cell LB handle the load difference created in neighboring cells.

Figure 5.22 shows the theoretically calculated number of unsatisfied users in Cell

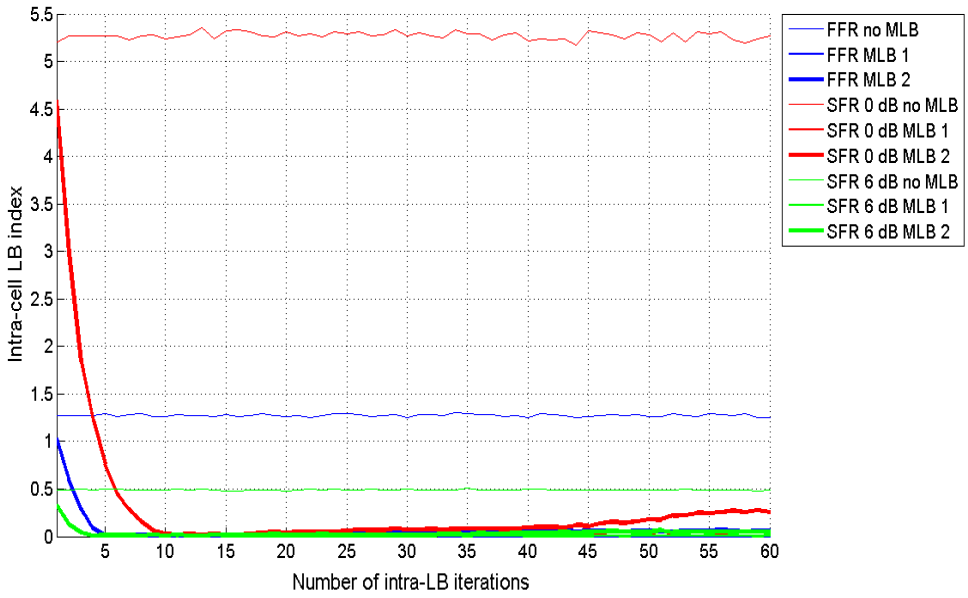

Figure 5.21. Intra-cell LB index varying load balancing iterations for Case 4.

1 for three system type for different frequency planning schemes for Case 4. Results show that in Case 4, number of unsatisfied users almost does change after MLB 1 for reuse-1, reuse-3. In the cases of SFR 6 dB and SFR 0 dB the gain of MLB 1 over no MLB system is about 35% however for FFR it is nearly 60%. After MLB 2, there is no unsatisfied users remain for FFR, SFR 0 dB and SFR 6 dB. In other words, Cell 1 is not overloaded anymore after MLB 2. On the other hand, in the case of reuse-1 30% of the users are still unsatisfied.

Figure 5.23, shows the ECDF of cell-edge user spectral efficiency of Cell 1 for round robin scheduler for Case 4. Without MLB cell-edge throughput reside between 0.3 - 0.5 bits/s/Hz. MLB 1 can not improve the cell-edge spectral efficiency for reuse-1 and reuse-3 since the surrounding cells are overloaded state with 35 users. On the other hand, it brings the minimum cell-edge spectral efficiency to between 0.66 - 0.92 bits/s/Hz for other frequency planning schemes for 50% of the cell-edge users. Additionally, MLB 2 brings the minimum cell-edge spectral efficiency to 0.50, 0.57 and 1 bits/s/Hz for reuse- 1, reuse-3 and SFR 0 dB, respectively whereas SFR 6 dB and FFR achieves the same minimum cell-edge spectral efficiency of 1.2 bits/s/Hz for 50% of the cell-edge users.

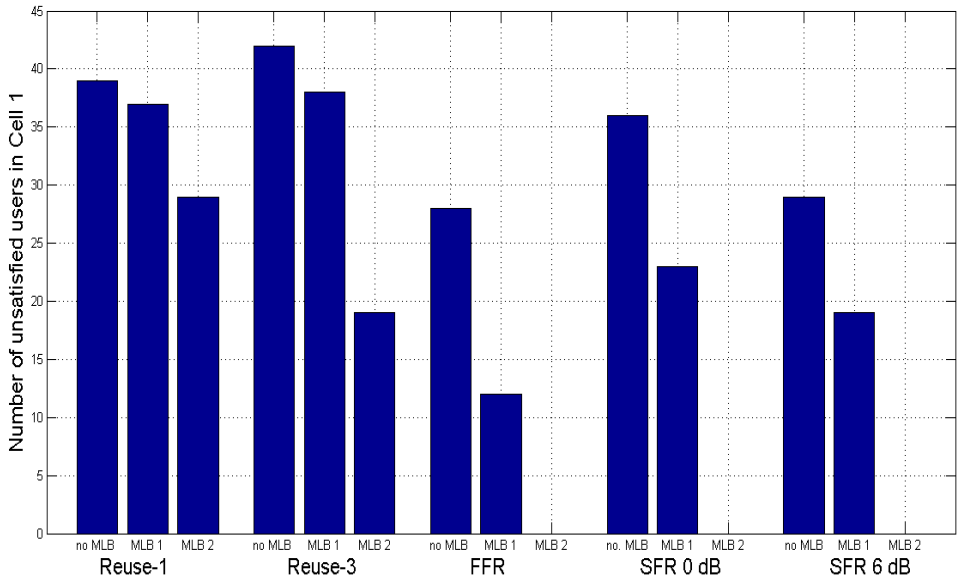

Figure 5.22. Number of unsatisfied users in Cell 1 for Case 4.

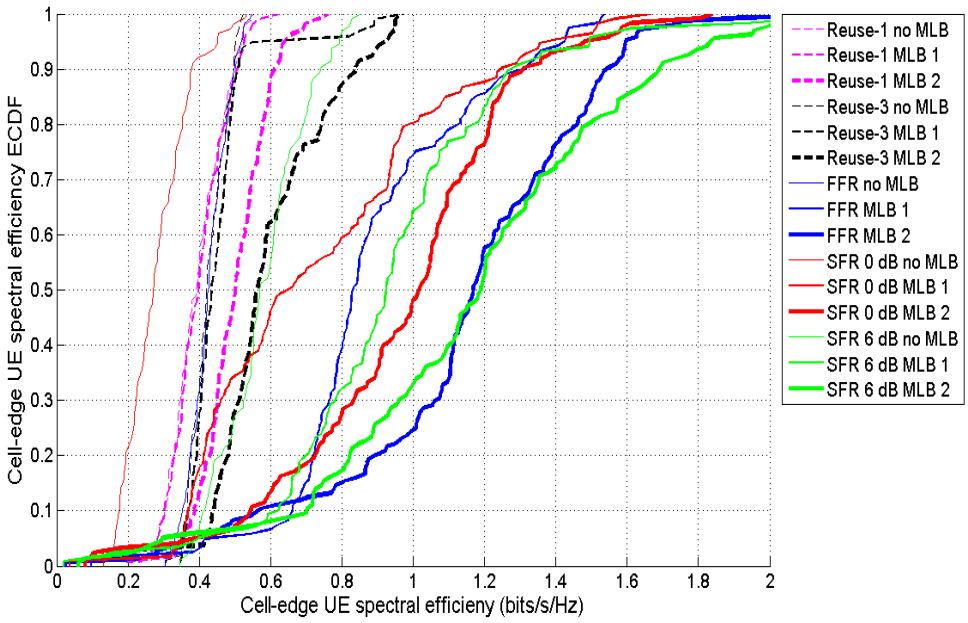

Figure 5.23. Performance of MLB with round-robin scheduler for different frequency planning schemes for Case 4.

Figure 5.24 compares the MLB performance of proportional fair for different frequency planning schemes for Case 4. Without MLB cell-edge spectral efficiency reside between 0.9 - 1.4 bits/s/Hz. As in round-robin scheduler MLB 1 can not improve the

cell-edge spectral efficiency for reuse-1 and reuse-3. However, for the other frequency planning schemes, it brings the minimum cell-edge spectral efficiency to between 1.8 - 2 bits/s/Hz for 50% of the cell-edge users. In the case of MLB 2, cell-edge spectral efficiency takes the values between 1.6 - 1.8 bits/s/Hz for reuse-1 and reuse-3 and between 2.2 - 2.5 bits/s/Hz for other frequency planning schemes. SFR 6 dB outperforms all the other frequency planning schemes in both MLB 1 and MLB 2. In more detail, without MLB 50% of the cell-edge users can not achieve more than 1.3 bits/s/Hz for SFR 6 dB, after MLB 1 and MLB 2 the minimum achievable spectral efficiency becomes 2 and 2.5 bits/s/Hz, respectively. In contrast, reuse-3 gives the lowest spectral efficiency after application of MLB techniques.

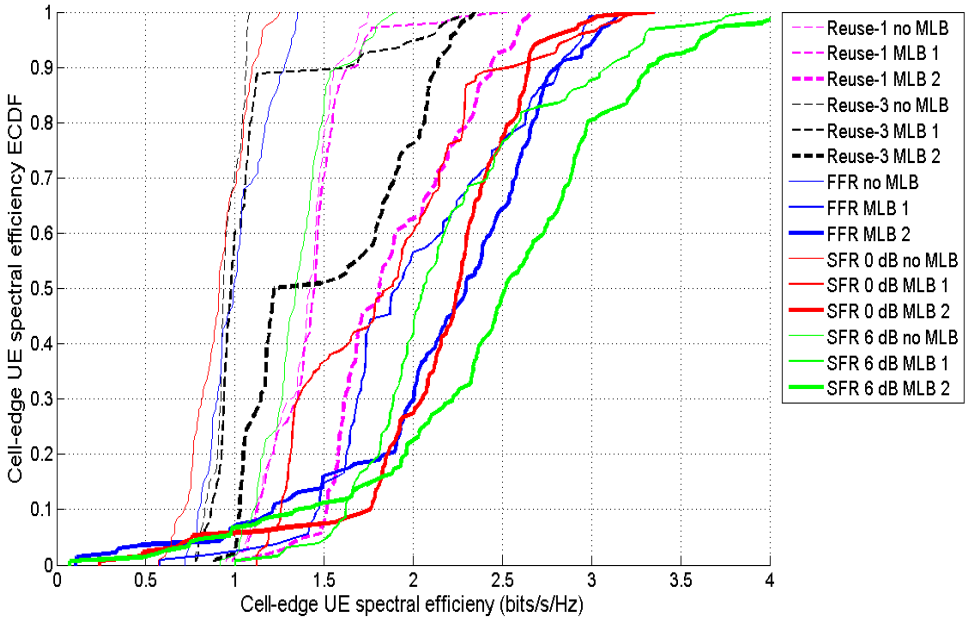

Figure 5.24. Performance of MLB with proportional fair scheduler for different frequency planning schemes for Case 4.

The results of Case 4 for the best-CQI scheduler for different frequency planning schemes are illustrated in Figure 5.25.

In Table 5.8, the mean bandwidth efficiency values of cell-edge users of Cell 1 for three system type are listed for different frequency schemes and for round-robin and proportional fair scheduler, respectively for Case 4. In Case 4, the adjacent neighbors

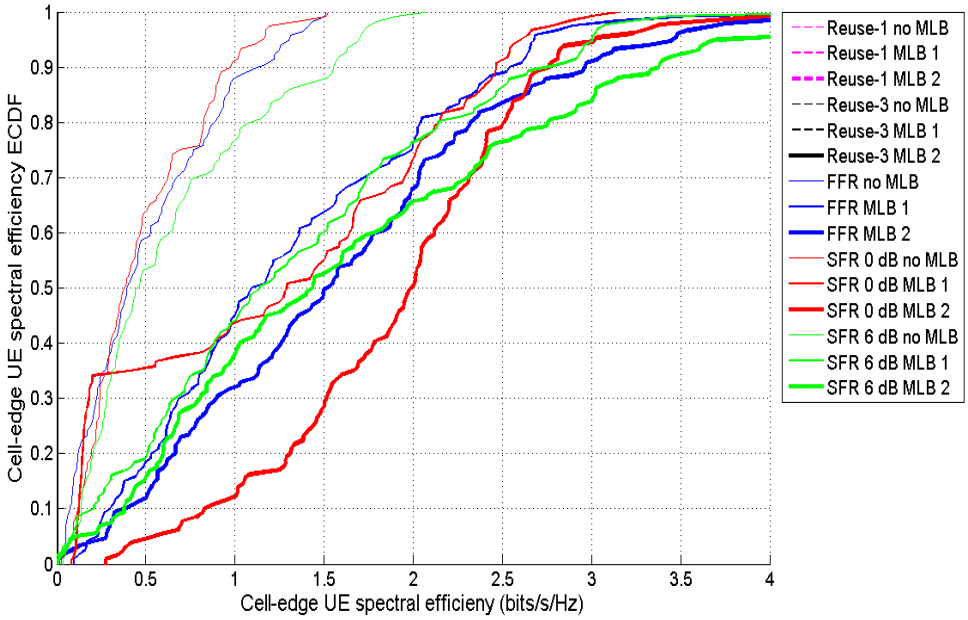

Figure 5.25. Performance of MLB with best-CQI scheduler for different frequency planning schemes for Case 4.

are overloaded and the improvement in the mean cell-edge spectral efficiency is very little after MLB 1 whereas the MLB 2 is really efficient. As in the previous cases, MLB 3 achieves less that MLB 1 and MLB 4 achieves less than MLB 2 in terms of cell-edge spectral efficiency. This result proves that coordination of intra-LB and inter-MLB is very efficient in the cases of FFR and SFR whereas Since for all four systems MLB refers inter-cell MLB for reuse-1 and reuse-3, the results are the same for MLB 1 and MLB 3 and for MLB 2 and MLB 4 for reuse-1 and reuse-3.

In Table 5.9, we can see the effect of MLB 1 and MLB 2 on the total system spectral efficiency in kbits/s/Hz for Case 4 for different frequency planning schemes and schedulers. In Case 4, MLB is also activated in overloaded adjacent neighbors of the central cell. Therefore, the degradation in total network spectral efficiency for Case 4 is more than the previous cases.

Table 5.8. Mean spectral efficiency of cell-edge users of Cell 1 in bits/s/Hz for Case 4 for different schedulers and frequency planning schemes.

		Reuse-1	Reuse-3	FFR	SFR 0 dB	SFR 6 dB
Round-robin scheduler	no MLB	0.39	0.42	0.46	0.29	0.53
	MLB 1	0.40	0.46	0.89	0.74	0.94
	MLB 2	0.50	0.60	1.15	0.97	1.16
	MLB 3	0.40	0.46	0.63	0.35	0.70
	MLB 4	0.50	0.60	0.65	0.48	0.70
Proportional fair scheduler	no MLB	1.42	0.96	0.97	0.90	1.38
	MLB 1	1.43	1.09	2.04	1.86	2.21
	MLB 2	1.90	1.5	2.17	2.17	2.47
	MLB 3	1.43	1.09	1.35	1.05	1.71
	MLB 4	1.90	1.5	1.40	1.46	1.74

Table 5.9. Total system spectral efficiency in kbits/s/Hz for Case 4 for different schedulers and frequency planning schemes.

		Reuse-1	Reuse-3	FFR	SFR 0 dB	SFR 6 dB
Round-Robin Scheduler	no MLB	1.88	1.04	1.68	2.06	1.85
	MLB 1	1.75	0.97	1.36	1.54	1.43
	MLB 2	1.66	0.94	1.29	1.50	1.35
Proportional fair Scheduler	no MLB	3.23	1.52	2.57	3.16	2.99
	MLB 1	3.10	1.42	2.26	2.57	2.47
	MLB 2	2.87	1.37	2.20	2.53	2.34
Best-CQI Scheduler	no MLB	4.65	1.65	2.88	3.65	3.63
	MLB 1	4.65	1.65	2.78	3.36	3.40
	MLB 2	4.65	1.65	2.74	3.33	3.33

5.2.5. Design Guideline

While designing a cellular network, the parameters which are optimized may vary depending on the network load and channel conditions. The type of scheduler

and frequency planning scheme affects the performance of the network. According to the results we observe in [48], round-robin and proportional fair schedulers optimize the mean throughput whereas best-CQI scheduling achieves highest peak throughput and sacrifices the cell-edge users. Additionally, the proportional fair scheduler performs better than the round-robin scheduler since it considers the channel conditions of the users. On the other hand, for static ICIC approaches which divide the cell into two regions, i.e. SFR and FFR, the radius of the interior region, the ratio of the allocated sub-carriers to the interior and exterior regions and the power factor used in SFR change the cell-edge and the peak throughput of the system. Therefore, these parameters should be selected carefully according to the design aspects.

MLB functionality directs the cell-edge users of overloaded cells to relatively less loaded cells to increase the spectral efficiency achieved by cell-edge users. When some of the cell-edge users are handedover, resources remain for the center users of overloaded cell increase therefore the mean spectral efficiency is expected to increase for the overloaded cell. In this section, we talk about on the design aspects according to MLB performance results.

Cell-edge user spectral efficiency: In this thesis, we compared the MLB performance achieved in the central cell with respect to the different load conditions in adjacent neighbors. For all cases, when we compare the round-robin and proportional fair scheduler, we observe that proportional fair scheduler achieves higher mean cell-edge spectral efficiency for all frequency planning schemes than the round-robin scheduler. For round-robin scheduler reuse-1 performs worst and FFR performs best among all frequency planning schemes. In the case of proportional fair scheduler, SFR 6 dB outperforms the other schemes while FFR is the second in terms of mean cell-edge spectral efficiency. When we compare the cases, it is observed that increasing number of users located in the surrounding cells decreases the gain of MLB 1 over no MLB but increases gain of MLB 2 over MLB 1. In Case 1, MLB 2 is not needed since the available capacity in the adjacent neighbors is enough to accommodate the excessive load of Cell 1. Especially, for Case 3 and 4, the improvement in terms of mean cell-edge spectral efficiency provided with MLB 1 is minimal for reuse-1 and reuse-3 since the

surrounding cells are in overloaded state with 30 and 35 users whereas considerable improvement is provided with FFR and SFR with cooperation of inter and intra-cell MLB. Under MLB 3 and MLB 4 only inter-MLB is executed for FFR and SFR so that the efficiency of intra-LB can observed when we compare MLB 3 and MLB 4 with MLB 1 and MLB 2, respectively. In best-CQI scheduling only a small number of user can be scheduled and there is a big gap between users in terms of allocated resources and achievable spectral efficiency therefore we do not list the values of mean spectral efficiency for best-CQI scheduler.

Total system spectral efficiency: After MLB, mean spectral efficiency of cell-edge users improves in the expense of a bit degradation total system spectral efficiency. According to the Table 5.3 to 5.9, it is observed that best-CQI scheduler gives the higher total system spectral efficiency since the peak spectral efficiency is maximized in best-CQI scheduling method. The other observation is that since reuse-1 uses the total bandwidth of the system without partitioning total system, total spectral efficiency is higher than the other frequency planning schemes although cell-edge spectral efficiency is less because of ICI.

Number of unsatisfied users: Results show that number of unsatisfied users is reduces when ICI is mitigated. The number of unsatisfied users is calculated based on the virtual state of the cell. Based on this situation, we understand that with the same number of users FFR create the minimum load among other methods. In some cases, for FFR and SFR 6 dB the theoretical number of unsatisfied users is less than the number of users which is achieved after MLB 2 for reuse-1 and reuse-3.

Intra-Cell LB index: Intra-cell LB index is minimized with FFR and SFR 6 dB and that indicates more balanced load distribution between the interior and exterior regions is achieved with FFR and SFR 6 dB deployments.

Inter-Cell LB index: Inter-cell LB index is maximized with FFR and SFR 6 dB and that indicates more balanced load distribution among the neighboring cells. Also it is observed that with the increasing number of users reside in adjacent neighboring

cells the inter-cell LB index improves with MLB 2.

6. CONCLUSION

In this thesis, we investigated the performance of MLB jointly with static ICIC approaches, i.e. FFR and SFR and for three different scheduling strategies, i.e. round-robin, proportional fair and best-CQI schedulers. The results are compared with the universal reuse factor and reuse-3 to show the efficiency different frequency planning schemes. In the cases of FFR and SFR, the intra-cell LB mechanism is included in MLB functionality together with inter-cell MLB. For each frequency planning scheme and scheduling strategies, it is observed that MLB improves system performance in terms of cell-edge spectral efficiency and number of unsatisfied users by providing more balanced load distributions among cells and between regions. In addition, it is shown that ICI mitigation techniques enhances the system performance more than the reuse-1 and reuse-3.

We configured two systems and in the first system only the adjacent neighbors of the overloaded cell is involved in MLB procedure whereas in the latter case non-adjacent neighbors are also included in the optimization area in the cases where there is no available capacity in the adjacent neighbors. We observe that as the number of users reside in the adjacent neighbors is increasing, the efficiency of including non-adjacent neighbors to the optimization area also increases. For both systems it is shown that proportional fair scheduler performs better than other schedulers in terms of mean cell-edge spectral efficiency. For proportional fair and round-robin scheduler, SFR 6 dB and FFR achieve higher cell-edge spectral efficiency the help of intra-LB additional to inter-cell MLB and also due to their ICI mitigation properties. On the other hand, it is observed that MLB is not effective for best-CQI scheduler since best-CQI scheduler maximizes peak spectral efficiency rather than cell-edge efficiency. Simulation results show that the improvement in the cell-edge spectral efficiency is realized in the expense of a bit degradation in total system spectral efficiency.

In the cases of SFR and FFR, we also show that when intra-LB is not involved in MLB operation the performance gain is very low compared to intra-cell and inter-MLB

cooperation. In other words, providing a balanced load distribution between inner and outer bands by modifying radius of the interior region increase the performance and spectral efficiency of cell-edge users. In this thesis, we consider MLB for static ICIC approaches and show the significant improvement in the performance metrics. There are also more advanced dynamic ICIC approaches. Performance of MLB could be considered jointly with dynamic ICIC approaches as a future work.

REFERENCES

1. Hämäläinen S., H. Sanneck and C. Sartori, *LTE Self-Organising Networks (SON): Network Management Automation for Operational Efficiency*, Wiley Publishing, New Jersey, 2011.

2. Dahlman, E., S. Parkvall, J. Sköld and P. Beming, *3G Evolution: HSPA and LTE for Mobile Broadband*, Academic Press, Boston, 2007.

3. Kumar, A., Y. Lui and J. Sengupta, "Evolution of Mobile Wireless Communication Networks: 1G to 4G", *International Journal of Electronics, Communication Technology*, pp. 2230-7109, 2010.

4. Astely, D., E. Dahlman, A. Furuskär, Y. Jading, M. Lindström and S. Parkvall, "LTE: The Evolution of Mobile Broadband", *IEEE Communications Magazine*, Vol. 47, No. 4, pp. 44-51, 2009.

5. 3GPP, "Requirements for Evolved UTRA (E-UTRA) and Evolved UTRAN (E-UTRAN) (Release 9)", TS 25.913, Tech Rep., 2009.

6. Alcatel-Lucent, *The LTE Network Architecture*, Strategic White Paper, 2009.

7. Holma, H. and A. Toskala, *LTE for UMTS OFDMA and SC-FDMA Based Radio Access*, Wiley Publishing, Chichester, 2009.

8. Goldsmith, A., *Wireless Communications*, Cambridge University Press, Chichester, 2005.

9. Sesia, S., M. Baker and I. Toufik, *LTE-The UMTS Long Term Evolution: From Theory to Practice*, Wiley Publishing, Chichester, 2009.

10. Lescuyer, P. and T. Lucidarme, *Evolved Packet System (EPS) - The LTE and SAE Evolution of 3G UMTS*, John Wiley and Sons Ltd., Chichester, 2008.

11. Agilent Technologies, *3GPP Long Term Evolution: System Overview, Product Development and Test Challenges*, White Paper, 2009.

12. 3GPP, "Physical layer procedures (Release 12)", TS 36.213, Tech. Rep., 2014.

13. Mehlführer, C., J. C. Ikuno, M. Simko, S. Schwarz, M. Wrulich and M. Rupp, "The Vienna LTE Simulators - Enabling Reproducibility in Wireless Communications Research", *EURASIP Journal on Advances in Signal Processing*, Tech. Rep., 2011.

14. NGMN, "NGMN Use Cases related to Self Organising Network, Overall Description", Tech. Rep., 2007.

15. Aliu, O. G., A. Imran, M. A. Imran and B. Evans, "A Survey of Self Organisation in Future Cellular Networks", *IEEE Communications Surveys and Tutorials*, Vol. 15, No. 1, pp. 336-361, 2013.

16. 3GPP, "Self-Configuring and Self-Optimizing Network Use Cases and Solutions (Release9)", TR 36.902, Tech. Rep., 2009.

17. 3GPP, "Telecommunications management; self-healing OAM; concepts and requirements (Release 10)", TS 32.541, Tech. Rep., 2010.

18. Seidel, E. and S. Feng,"Self-Organizing Networks (SON) in 3GPP Long Term Evolution", Nomor Research GmbH, Tech. Rep., 2008.

19. 3GPP, "Radio Resource Control (RRC): Protocol Specification (Release 11)", TR 36.331, Tech. Rep., 2012.

20. Viering, I., M. Döttling and A. Lobinger, "A Mathematical Perspective of Self-Optimizing Wireless Networks", *IEEE International Conference on Communications*, pp. 1-6, 2009.

21. 3GPP, "Self-Organizing Networks (SON) Policy Network Resource Model

(NRM) Integration Reference Point (IRP) Information Service (Release 11)", TS 32.522, Tech. Rep., 2013.

22. Zia, N. and A. Mitschele-Thiel, "Self-Organized Neighborhood Mobility Load Balancing for LTE Networks", *2013 IFIP Wireless Days*, pp. 1-6, 2013.

23. Lobinger, A., S. Stefanski, T. Jansen and I. Balan, "Load Balancing in Downlink LTE Self-Optimizing Networks, *in Proc. IEEE 71st Vehicular Technology Conference*, pp. 1-5, 2010.

24. Yang, Y., P. Li, X. Chen, and W. Wang, "A High-Efficient Algorithm of Mobile Load Balancing in LTE System", *in Proc. IEEE Vehicular Technology Conference*, pp. 1-5, 2012.

25. Lv, W., W. Li, H. Zhang and Y. Liu, "Distributed Mobility Load Balancing with RRM in LTE", *3rd IEEE International Conference on Broadband Network and Multimedia Technology*, pp. 457-461, 2010.

26. Wang, H., L. Ding, P. Wu, Z. Pan, N. Liu, X. You and Z. Li, "A Unified Algorithm for Mobility Load Balancing in 3GPP LTE Multi-Cell Networks", *Science China*, Vol. 1, No. 12, pp. 1-11, 2012.

27. Wang, H., L. Ding, P. Wu, Z. Pan, N. Liu and X. You, "Dynamic Load Balancing in 3GPP LTE Multi-Cell Networks with Heterogenous Services", *5th International ICST Conference on Communications and Networking in China*, pp. 1-5, 2010.

28. Li, Z., H. Wang, Z. Pan, N. Liu and X. You, "Joint Optimization on Load Balancing and Network Load in 3GPP LTE Multi-Cell Networks", *International Conference on Wireless Communications and Signal Processing*, pp. 1-5, 2011.

29. Zhang, L., Y. Liu, M. Zhang, S. Jia and X. Duan, "A Two-Layer Mobility Load Balancing in LTE Self-Organization Networks", *IEEE 13th International*

Conference on Communication Technology, pp. 925-929, 2011.

30. Suga, J., Y. Kojima and M. Okuda, "Centralized Mobility Load Balancing Scheme in LTE Systems", *8th International Symposium on Wireless Communication Systems*, pp. 306-310, 2011.

31. Wei, Y. and M. Peng, "A Mobility Load Balancing Optimization Method for Hybrid Architecture in Self-Organizing Network", *IET International Conference on Communication Technology and Application*, pp. 828-838, 2010.

32. Liu, Z., P. Hong, K. Xue and M. Peng, "Conflict Avoidance between Mobility Robustness Optimization and Mobility Load Balancing", *IEEE Global Telecommunications Conference*, pp. 1-5, 2010.

33. Li, Y., M. Li, B. Cao and W. Liu, "A Conflict Avoid Method between Load Balancing and Mobility Robustness Optimization in LTE", *1st IEEE International Conference on Communications in China*, pp. 143-148, 2012.

34. Dahlman, E., S. Parkvall and J. Sköld, *4G: LTE/LTE Advanced for Mobile Broadband*, Academic Press, Boston, 2011.

35. Mengistie, W. A. and K. Ronoh, *Load Balancing in Heterogeneous LTE-A Networks*, M.S. Thesis, Linkpings University, 2012.

36. Warabino, T., S. Kaneko, S. Nanba and Y. Kishi, "Advanced Load Balancing in LTE/LTE-A Cellular Network", *23rd IEEE International Symposium on Personal Indoor and Mobile Radio Communications*, pp. 530-535, 2012.

37. Son, K., S. Chong and G. Veciana, "Dynamic Association for Load Balancing and Interference Avoidance in Multi-Cell Networks", *IEEE Transactions on Wireless Communications*, Vol. 8, No. 7, pp. 3566-3576, 2009.

38. Li, Z., H. Wang, Z. Pan, N. Liu and Xiaohu You, "Dynamic Load Balancing in 3GPP LTE Multi-Cell Fractional Frequency Reuse Networks", *IEEE Vehicular*

Technology Conference, Vol. 1, No. 5, pp. 3-6, 2012.

39. Khan, F., *LTE for 4G Mobile Broadband, Air Interface Technologies and Performance*, Cambridge University Press, Cambridge, 2009.

40. Iosif, O. and I. Banica, "On the Analysis of Packet Scheduling in Downlink 3GPP LTE System", *in Proc of the 4th International Conference on Communication Theory, Reliability and Quality of Service*, pp. 99-102, 2011.

41. Dikamba, T., *Downlink Scheduling in 3GPP Long Term Evolution (LTE)*, M.S. Thesis, Delft University of Technology, 2011.

42. Kawser, M., H. Farid, A. Hasin, A. Sadik and I. Razu, "Performance Comparison between Round Robin and Proportional Fair Scheduling Methods for LTE", *International Journal of Information and Electronics Engineering*, Vol. 2, No. 5, pp. 678-681, 2012.

43. AlQahtani, S. A. and M. Alhassany, "Comparing Different LTE Scheduling Schemes", *9th International Wireless Communications and Mobile Computing Conference*, pp. 264-269, 2013.

44. Elsayed, K., "4G++: Advanced Performance Boosting Techniques in 4th Generation Wireless Systems and Beyond", *The First NTRA Knowledge Dissemination and Networking Conference*, Tech. Rep., 2011.

45. Boudreau, G., J. Panicker, N. Guo, R. Chang, N. Wang and S. Vrzic, "Interference Coordination and Cancellation for 4G Networks", *IEEE Communications Magazine*, Vol. 47, No. 4, pp. 74-81, 2009.

46. Novlan, T., J. G. Andrews, Illsoo Sohn, R.K. Ganti and A. Ghosh, "Comparison of Fractional Frequency Reuse Approaches in OFDMA Cellular Downlink", *IEEE Global Telecommunications Conference (GLOBECOM 2010)*, pp. 1-5, 2010.

47. Huawei, "R1-050507: Soft Frequency Reuse Scheme for UTRAN LTE, 3GPP TSG RAN WG1 Meeting 41, Tech. Rep., 2005.

48. Gok, A. and M. Koca, "Performance evaluation of frequency planning and scheduling schemes in OFDMA Networks", *IEEE International Black Sea Conference on Communications and Networking*, pp. 149-153, 2014.